Table 7: Allele Frequencies of ABCB1 SNPs Investigated in This Study[a]

position and change					wild type		variant type		
amino acid	cDNA		ethnic group	no. of samples	allele	frequency (%)	allele	frequency (%)	ref
S400N	1199	G > A	African	111	G	100.0	A	0.0	*23*
			African-American	100	G	99.0	A	1.0	*16*
			German	461	G	94.5	A	5.5	*29*
			Caucasian	85	G	87.1	A	12.9	*6*
			Caucasian	50	G	98.0	A	2.0	*31*
			Caucasian	100	G	97.5	A	2.5	*16*
			Mexican-American	10	G	100.0	A	0.0	*16*
			Asian-American	30	G	100.0	A	0.0	*16*
			Pacific Islander	7	G	100.0	A	0.0	*16*
R492C	1474	C > T	African-American	23	C	100.0	T	0.0	*7*
			Caucasian	37	C	98.6	T	1.4	*7*
R669C	2005	C > T	African-American	100	C	99.0	T	1.0	*16*
			Caucasian	100	C	100.0	T	0.0	*16*
			Mexican-American	10	C	100.0	T	0.0	*16*
			Asian-American	30	C	100.0	T	0.0	*16*
			Pacific Islander	7	C	100.0	T	0.0	*16*
I849M	2547	A > G	African-American	100	C	100.0	T	0.0	*16*
			Caucasian	100	C	99.5	T	0.5	*16*
			Mexican-American	10	C	100.0	T	0.0	*16*
			Asian-American	30	C	100.0	T	0.0	*16*
			Pacific Islander	7	C	100.0	T	0.0	*16*
A893P/S/T	2677	G > T/A/C	African (Beninese)	111	G	99.1	T	0.9	*23*
							A	0.0	
			African-American	100	G	89.5	T	10.0	*16*
							A	0.5	
			Caucasian	100	G	50.0	T	46.5	*16*
							A	3.5	
			Caucasian	50	G	52.0	T	38.0	*31*
							A	10.0	
			German	461	G	56.5	T	41.6	*29*
							A	1.9	
			Mexican-American	10	G	60.0	T	40.0	*16*
							A	0.0	
			Asian-American	30	G	33.3	T	45.0	*16*
							A	21.7	
			Japanese	117	G	44.0	T	35.5	*8*
							A	20.5	
			Japanese (placenta)	100	G	43.0	T	39.0	*30*
							A	18.0	
			Japanese	48	G	36.5	T	41.7	*30*
							A	21.8	
			Pacific Islander	7	G	28.6	T	35.7	*16*
							A	35.7	
			ND	ND	G	ND	C	ND	NCBI dbSNP (rs2032582)
M986V	2956	A > G	Japanese (placenta)	100	A	99.5	G	0.5	*30*
			Japanese	48	A	100.0	G	0.0	*30*
A999T	2995	G > A	cell lines	36	G	94.4	A	5.6	*28*
P1051A	3151	C > G	African-American	100	C	99.5	G	0.5	*16*
			Caucasian	100	C	100.0	G	0.0	*16*
			Mexican-American	10	C	100.0	G	0.0	*16*
			Asian-American	30	C	100.0	G	0.0	*16*
			Pacific Islander	7	C	100.0	G	0.0	*16*
G1063A	3188	G > A	ND	ND	G	ND	A	ND	NCBI dbSNP (rs2707944)

[a] ND, not determined.

structures. Markush TOPFRAG is the software that generates the CFCs from chemical structure information.

The uniqueness of this approach derives from the fact that ABCB1 ATPase activity is described as a linear combination of CFCs and that the coefficient for each CFC reflects the extent of the contribution of a specific chemical moiety to the ATPase activity. As demonstrated in Table 5 and Figure 7, there is a large variation among the SNP variants in terms of the CFCs contributing to the ATPase activity, suggesting that nonsynonymous polymorphisms influence the substrate specificity of ABCB1 (Table. 6). The point in the catalytic cycle at which substrate binding takes place and details of how ATP hydrolysis drives transport may be critical for understanding the mechanism of substrate specificity (*51*).

Concluding Remarks The effect of SNPs on the transport activity appears to depend on the substrates tested, and therefore the functional analysis of SNPs by using a wide variety of substrates is of great interest. This concept was verified by our recent study on the genetic polymorphisms of human ABCG2 (*52*, *53*). One amino acid substitution can alter interactions between the active site of an ABC transporter and substrate molecules. Therefore, it is critically

important to quantitatively analyze and evaluate such structure-related interactions. In this context, the new QSAR analysis with CFCs will provide a powerful tool to quantify the impact of genetic polymorphisms on the function of ABC transporters. If the chemical structure of a test compound is available, we are able to predict the effect of SNPs on the substrate specificity of ABCB1 toward the compound by using our QSAR analysis method. The validity of our QSAR analysis method was proven in our recent studies where troglitazone and gefitinib were predicted to be strong inhibitors for ABCB11 (*54*) and ABCG2 (*55*), respectively. It is also possible to further expand this QSAR analysis with a larger number of structurally unrelated compounds, if needed.

ACKNOWLEDGMENT

The first and second authors equally contributed to this study. The authors thank Drs. Deanna L. Kroetz and Kathleen M. Giacomini (Department of Biopharmaceutical Sciences, University of California San Francisco, San Francisco, CA) for their kind advice on the haplotype in the human *ABCB1* gene.

REFERENCES

1. Ambudkar, S. V., Lelong, I. H., Zhang, J., and Cardarelli, C. (1998) Purification and reconstitution of human P-glycoprotein, *Methods Enzymol. 292*, 492−504.
2. Gottesman, M. M., and Ling, V. (2006) The molecular basis of multidrug resistance in cancer: the early years of P-glycoprotein research, *FEBS Lett. 580*, 998−1009.
3. Schinkel, A. H., Smit, J. J., van Tellingen, O., Beijnen, J. H., Wagenaar, E., van Deemter, L., Mol, C. A., van der Valk, M. A., Robanus-Maandag, E. C., te Riele, H. P. J., Bernsd, A. J. M., and Borst, P. (1994) Disruption of the mouse mdr1a P-glycoprotein gene leads to a deficiency in the blood-brain barrier and to increased sensitivity to drugs, *Cell 77*, 491−502.
4. Virgintino, D., Robertson, D., Errede, M., Benagiano, V., Tauer, U., Roncali, L., and Bertossi, M. (2002) Expression of caveolin-1 in human brain microvessels, *Neuroscience 115*, 145−152.
5. Kerb, R., Hoffmeyer, S., and Brinkmann, U. (2001) ABC drug transporters: hereditary polymorphisms and pharmacological impact in MDR1, MRP1 and MRP2, *Pharmacogenomics 2*, 51−64.
6. Hoffmeyer, S., Burk, O., von Richter, O., Arnold, H. P., Brockmoller, J., Johne, A., Cascorbi, I., Gerloff, T., Roots, I., Eichelbaum, M., and Brinkmann, U. (2000) Functional polymorphisms of the human multidrug-resistance gene: multiple sequence variations and correlation of one allele with P-glycoprotein expression and activity in vivo, *Proc. Natl. Acad. Sci. U.S.A. 97*, 3473−3478.
7. Kim, R. B., Leake, B. F., Choo, E. F., Dresser, G. K., Kubba, S. V., Schwarz, U. I., Taylor, A., Xie, H. G., McKinsey, J., Zhou, S., Lan, L. B., Schuetz, J. D., Schuetz, E. G., and Wilkinson, G. R. (2001) Identification of functionally variant MDR1 alleles among European Americans and African Americans, *Clin. Pharmacol. Ther. 70*, 189−199.
8. Horinouchi, M., Sakaeda, T., Nakamura, T., Morita, Y., Tamura, T., Aoyama, N., Kasuga, M., and Okumura, K. (2002) Significant genetic linkage of MDR1 polymorphisms at positions 3435 and 2677: functional relevance to pharmacokinetics of digoxin, *Pharm. Res. 19*, 1581−1585.
9. Itoda, M., Saito, Y., Komamura, K., Ueno, K., Kamakura, S., Ozawa, S., and Sawada, J. (2002) Twelve novel single nucleotide polymorphisms in ABCB1/MDR1 among Japanese patients with ventricular tachycardia who were administered amiodarone, *Drug Metab. Pharmacokinet. 17*, 566−571.
10. Johne, A., Kopke, K., Gerloff, T., Mai, I., Rietbrock, S., Meisel, C., Hoffmeyer, S., Kerb, R., Fromm, M. F., Brinkmann, U., Eichelbaum, M., Brockmoller, J., Cascorbi, I., and Roots, I. (2002) Modulation of steady-state kinetics of digoxin by haplotypes of the P-glycoprotein MDR1 gene, *Clin. Pharmacol. Ther. 72*, 584−594.
11. Macphee, I. A., Fredericks, S., Tai, T., Syrris, P., Carter, N. D., Johnston, A., Goldberg, L., and Holt, D. W. (2002) Tacrolimus pharmacogenetics: polymorphisms associated with expression of cytochrome p4503A5 and P-glycoprotein correlate with dose requirement, *Transplantation 74*, 1486−1489.
12. Saito, S., Iida, A., Sekine, A., Miura, Y., Ogawa, C., Kawauchi, S., Higuchi, S., and Nakamura, Y. (2002) Three hundred twenty-six genetic variations in genes encoding nine members of ATP-binding cassette, subfamily B (ABCB/MDR/TAP), in the Japanese population, *J. Hum. Genet. 47*, 38−50.
13. Siegmund, W., Ludwig, K., Giessmann, T., Dazert, P., Schroeder, E., Sperker, B., Warzok, R., Kroemer, H. K., and Cascorbi, I. (2002) The effects of the human MDR1 genotype on the expression of duodenal P-glycoprotein and disposition of the probe drug talinolol, *Clin. Pharmacol. Ther. 72*, 572−583.
14. Evans, W. E., and McLeod, H. L. (2003) Pharmacogenomics−drug disposition, drug targets, and side effects, *N. Engl. J. Med. 348*, 538−549.
15. Kafka, A., Sauer, G., Jaeger, C., Grundmann, R., Kreienberg, R., Zeillinger, R., and Deissler, H. (2003) Polymorphism C3435T of the MDR-1 gene predicts response to preoperative chemotherapy in locally advanced breast cancer, *Int. J. Oncol. 22*, 1117−1121.
16. Kroetz, D. L., Pauli-Magnus, C., Hodges, L. M., Huang, C. C., Kawamoto, M., Johns, S. J., Stryke, D., Ferrin, T. E., DeYoung, J., Taylor, T., Carlson, E. J., Herskowitz, I., Giacomini, K. M., and Clark, A. G. (2003) Sequence diversity and haplotype structure in the human ABCB1 (MDR1, multidrug resistance transporter) gene, *Pharmacogenetics 13*, 481−494.
17. Saito, K., Miyake, S., Moriya, H., Yamazaki, M., Itoh, F., Imai, K., Kurosawa, N., Owada, E., and Miyamoto, A. (2003) Detection of the four sequence variations of MDR1 gene using TaqMan MGB probe based real-time PCR and haplotype analysis in healthy Japanese subjects, *Clin. Biochem. 36*, 511−518.
18. Sakaeda, T., Nakamura, T., and Okumura, K. (2003) Pharmacogenetics of MDR1 and its impact on the pharmacokinetics and pharmacodynamics of drugs, *Pharmacogenomics 4*, 397−410.
19. Weinshilboum, R. (2003) *N. Engl. J. Med.*, 529−537.
20. Marzolini, C., Paus, E., Buclin, T., and Kim, R. B. (2004) Polymorphisms in human MDR1 (P-glycoprotein): recent advances and clinical relevance, *Clin. Pharmacol. Ther. 75*, 13−33.
21. Ozawa, S., Soyama, A., Saeki, M., Fukushima-Uesaka, H., Itoda, M., Koyano, S., Sai, K., Ohno, Y., Saito, Y., and Sawada, J. (2004) Ethnic differences in genetic polymorphisms of CYP2D6, CYP2C19, CYP3As and MDR1/ABCB1, *Drug Metab. Pharmacokinet. 19*, 83−95.
22. Uwai, Y., Masuda, S., Goto, M., Motohashi, H., Saito, H., Okuda, M., Nakamura, E., Ito, N., Ogawa, O., and Inui, K. (2004) Common single nucleotide polymorphisms of the MDR1 gene have no influence on its mRNA expression level of normal kidney cortex and renal cell carcinoma in Japanese nephrectomized patients, *J. Hum. Genet. 49*, 40−45.
23. Allabi, A. C., Horsmans, Y., Issaoui, B., and Gala, J. L. (2005) Single nucleotide polymorphisms of ABCB1 (MDR1) gene and distinct haplotype profile in a West Black African population, *Eur. J. Clin. Pharmacol. 61*, 97−102.
24. Sakurai, A., Tamura, A., Onishi, Y., and Ishikawa, T. (2005) Genetic polymorphisms of ATP-binding cassette transporters ABCB1 and ABCG2: therapeutic implications, *Expert Opin. Pharmacother. 6*, 2455−2473.
25. Sakaeda, T. (2005) MDR1 genotype-related pharmacokinetics: fact or fiction?, *Drug Metab. Pharmacokinet. 20*, 391−414.
26. Green, H., Soderkvist, P., Rosenberg, P., Horvath, G., and Peterson, C. (2006) mdr-1 single nucleotide polymorphisms in ovarian cancer tissue: G2677T/A correlates with response to paclitaxel chemotherapy, *Clin. Cancer Res. 12*, 854−849.
27. Kimchi-Sarfaty, C., Oh, J. M., Kim, I. W., Sauna, Z. E., Calcagno, A. M., Ambudkar, S. V., and Gottesman, M. M. (2007) A "silent" polymorphism in the MDR1 gene changes substrate specificity, *Science 315*, 525−528.
28. Mickley, L. A., Lee, J. S., Weng, Z., Zhan, Z., Alvarez, M., Wilson, W., Bates, S. E., and Fojo, T. (1998) Genetic polymorphism in MDR-1: a tool for examining allelic expression in normal cells, unselected and drug-selected cell lines, and human tumors, *Blood 91*, 1749−1756.
29. Cascorbi, I., Gerloff, T., Johne, A., Meisel, C., Hoffmeyer, S., Schwab, M., Schaeffeler, E., Eichelbaum, M., Brinkmann, U., and Roots, I. (2001) Frequency of single nucleotide polymorphisms

in the P-glycoprotein drug transporter MDR1 gene in white subjects, *Clin. Pharmacol. Ther. 69*, 169−174.
30. Tanabe, M., Ieiri, I., Nagata, N., Inoue, K., Ito, S., Kanamori, Y., Takahashi, M., Kurata, Y., Kigawa, J., Higuchi, S., Terakawa, N., and Otsubo, K. (2001) Expression of P-glycoprotein in human placenta: relation to genetic polymorphism of the multidrug resistance (MDR)-1 gene, *J. Pharmacol. Exp. Ther. 297*, 1137−1143.
31. Gerloff, T., Schaefer, M., Johne, A., Oselin, K., Meisel, C., Cascorbi, I., and Roots, I. (2002) MDR1 genotypes do not influence the absorption of a single oral dose of 1 mg digoxin in healthy white males, *Br. J. Clin. Pharmacol. 54*, 610−616.
32. Ishikawa, T., Sakurai, A., Kanamori, Y., Nagakura, M., Hirano, H., Takarada, Y., Yamada, K., Fukushima, K., and Kitajima, M. (2005) High-speed screening of human ATP-binding cassette transporter function and genetic polymorphisms: new strategies in pharmacogenomics, *Methods Enzymol. 400*, 485−510.
33. Sarkadi, B., Price, E. M., Boucher, R. C., Germann, U. A., and Scarborough, G. A. (1992) Expression of the human multidrug resistance cDNA in insect cells generates a high activity drug-stimulated membrane ATPase, *J. Biol. Chem. 267*, 4854−4858.
34. Onishi, Y., Hirano, H., Nakata, K., Oosumi, K., Nagakura, M., Tarui, S., and Ishikawa, T. (2003) High-speed screening and structure-activity relationship analysis for the substrate specificity of P-glycoprotein (ABCB1), *Chem-Bio Inf. J. 3*, 175−193.
35. Thompson, J. D., Gibson, T. J., Plewniak, F., Jeanmougin, F., and Higgins, D. G. (1997) The CLUSTAL_X windows interface: flexible strategies for multiple sequence alignment aided by quality analysis tools, *Nucleic Acids Res. 25*, 4876−4882.
36. Sali, A., and Blundell, T. L. (1993) Comparative protein modelling by satisfaction of spatial restraints, *J. Mol. Biol. 234*, 779−815.
37. Dawson, R. J., and Locher, K. P. (2006) Structure of a bacterial multidrug ABC transporter, *Nature 443*, 180−185.
38. Hrycyna, C. A., Airan, L. E., Germann, U. A., Ambudkar, S. V., Pastan, I., and Gottesman, M. M. (1998) Structural flexibility of the linker region of human P-glycoprotein permits ATP hydrolysis and drug transport, *Biochemistry 37*, 13660−13673.
39. Fiser, A., Do, R. K., and Sali, A. (2000) Modeling of loops in protein structures, *Protein Sci. 9*, 1753−1773.
40. Vriend, G. (1990) WHAT IF: a molecular modeling and drug design program, *J. Mol. Graphics 8*, 52−56.
41. Laskowski, R. A., MacArthur, M. W., Moss, D. S., and Thornton, J. M. (1993) PROCHECK: a program to check the stereochemical quality of protein structures, *J. Appl. Crystallogr. 26*, 283−291.
42. Case, D. A., Darden, T. A., Cheatham, T. E., III, Simmerling, C. L., Wang, J., Duke, R. E., Luo, R., Merz, K. M., Wang, B., Pearlman, D. A., Crowley, M., Brozell, S., Tsui, V., Gohlke, H., Mongan, J., Hornak, V., Cui, G., Beroza, P., Schafmeister, C., Caldwell, J. W., Ross, W. S., and Kollman, P. A. (2004) University of California, San Francisco.
43. Onufriev, A., Bashford, D., and Case, D. A. (2000) Modification of the generalized Born model suitable for macromolecules, *J. Phys. Chem. B 104*, 3712−3720.
44. Berendsen, H. J. C., Postma, J. P. M., van Gunsteren, W. F., DiNola, A., and Haak, J. R. (1984) Molecular dynamics with coupling to an external bath, *J. Chem. Phys. 81*, 3684−3690.
45. Ryckaert, J., Ciccotti, G., and Berendsen, H. J. C. (1977) Numerical integration of the cartesian equations of motion of a system with constraints: molecular dynamics of *n*-alkanes, *J. Comput. Phys. 23*, 327−341.
46. Georges, E., Bradley, G., Gariepy, J., and Ling, V. (1990) Detection of P-glycoprotein isoforms by gene-specific monoclonal antibodies, *Proc. Natl. Acad. Sci. U.S.A. 87*, 152−156.
47. Ishikawa, T., Tamura, A., Saito, H., Wakabayashi, K., and Nakagawa, H. (2005) Pharmacogenomics of the human ABC transporter ABCG2: from functional evaluation to drug molecular design, *Naturwissenschaften 92*, 451−463.
48. Yoshiura, K., Kinoshita, A., Ishida, T., Ninokata, A., Ishikawa, T., Kaname, T., Bannai, M., Tokunaga, K., Sonoda, S., Komaki, R., Ihara, M., Saenko, V. A., Alipov, G. K., Sekine, I., Komatsu, K., Takahashi, H., Nakashima, M., Sosonkina, N., Mapendano, C. K., Ghadami, M., Nomura, M., Liang, D. S., Miwa, N., Kim, D. K., Garidkhuu, A., Natsume, N., Ohta, T., Tomita, H., Kaneko, A., Kikuchi, M., Russomando, G., Hirayama, K., Ishibashi, M., Takahashi, A., Saitou, N., Murray, J. C., Saito, S., Nakamura, Y., and Niikawa, N. (2006) A SNP in the ABCC11 gene is the determinant of human earwax type, *Nat. Genet. 38*, 324−330.
49. Gervasini, G., Carrillo, J. A., Garcia, M., San Jose, C., Cabanillas, A., and Benitez, J. (2006) Adenosine triphosphate-binding cassette B1 (ABCB1) (multidrug resistance 1) G2677T/A gene polymorphism is associated with high risk of lung cancer, *Cancer 107*, 2850−2857.
50. Loo, T. W., Bartlett, M. C., and Clarke, D. M. (2005) ATP hydrolysis promotes interactions between the extracellular ends of transmembrane segments 1 and 11 of human multidrug resistance P-glycoprotein, *Biochemistry 44*, 10250−10258.
51. Ambudkar, S. V., Kim, I. W., and Sauna, Z. E. (2006) The power of the pump: Mechanisms of action of P-glycoprotein (ABCB1), *Eur. J. Pharm. Sci. 27*, 392−400.
52. Tamura, A., Watanabe, M., Saito, H., Nakagawa, H., Kamachi, T., Okura, I., and Ishikawa, T. (2006) Functional validation of the genetic polymorphisms of human ATP-binding cassette (ABC) transporter ABCG2: identification of alleles that are defective in porphyrin transport, *Mol. Pharmacol. 70*, 287−296.
53. Tamura, A., Wakabayashi, K., Onishi, Y., Takeda, M., Ikegami, Y., Sawada, S., Tsuji, M., Matsuda, Y., and Ishikawa, T. (2007) Re-evaluation and functional classification of non-synonymous single nucleotide polymorphisms of the human ATP-binding cassette transporter ABCG2, *Cancer Sci. 98*, 231−239.
54. Hirano, H., Kurata, A., Onishi, Y., Sakurai, A., Saito, H., Nakagawa, H., Nagakura, M., Tarui, S., Kanamori, Y., Kitajima, M., and Ishikawa, T. (2006) High-speed screening and QSAR analysis of human ATP-binding cassette transporter ABCB11 (bile salt export pump) to predict drug-induced intrahepatic cholestasis, *Mol. Pharmaceutics 3*, 252−265.
55. Saito, H., Hirano, H., Nakagawa, H., Fukami, T., Oosumi, K., Murakami, K., Kimura, H., Kouchi, T., Konomi, M., Tao, E., Tsujikawa, N., Tarui, S., Nagakura, M., Osumi, M., and Ishikawa, T. (2006) A new strategy of high-speed screening and quantitative structure-activity relationship analysis to evaluate human ATP-binding cassette transporter ABCG2-drug interactions, *J. Pharmacol. Exp. Ther. 317*, 1114−1124.

BI700330B

J Hum Genet (2007) 52:686–689
DOI 10.1007/s10038-007-0165-y

A Japanese patient with a mild Lenz–Majewski syndrome

Sumito Dateki · Tatsuro Kondoh · Gen Nishimura · Katsuaki Motomura · Koh-ichiro Yoshiura · Akira Kinoshita · Hideo Kuniba · Yoshiyuki Koga · Hiroyuki Moriuchi

Received: 10 April 2007 / Accepted: 17 May 2007 / Published online: 26 June 2007

Abstract We report on a sclerosing bone dysplasia, associated with cutis laxa, enamel dysplasia, and mental retardation. The patient was a 17-year-old Japanese boy of normal height and muscular build. Cutis laxa with prominent veins in the scalp and abdominal wall and delayed eruption of permanent teeth attracted the attention of clinicians in infancy and adolescence, respectively. The clinical manifestations included a progeroid facial appearance with prognathism, wrinkled skin, and interdigital webbing. The intelligence quotient was estimated at 60. Enamel dysplasia was histologically confirmed. Skeletal changes included calvarial hyperostosis, sclerosis of the skull base, an enlarged, sclerotic mandible, broad clavicles and ribs, and diaphyseal undermodeling of the tubular bones. Metaepiphyseal sclerosis or longitudinal striation was found in the long bones. Metaphyseal equivalents of the axial skeleton showed dense osteosclerosis. These clinical and radiological manifestations overlapped with those of Lenz–Majewski syndrome. Unlike the classical phenotype of the disorder, however, he did not show brachymesophalangy with proximal symphalangism or growth failure. The present case may be considered to fall in the mildest end in the phenotypic continuum of Lenz–Majewski syndrome, suggesting that the clinical spectrum of the disorder may be broader than currently thought.

Keywords Cranial sclerosis · Cutis laxa · Lenz–Majewski syndrome · Mental retardation · Progeria

S. Dateki (✉) · T. Kondoh · K. Motomura · H. Moriuchi
Department of Pediatrics,
Nagasaki University Graduate School of Biomedical Sciences,
1-7-1, Sakamoto, Nagasaki 852-8501, Japan
e-mail: sum826@net.nagasaki-u.ac.jp

G. Nishimura
Department of Radiology, Tokyo Metropolitan Kiyose Children's Hospital, Tokyo, Japan

K. Yoshiura · A. Kinoshita · H. Kuniba
Department of Human Genetics,
Nagasaki University Graduate School of Biomedical Sciences, Nagasaki, Japan

Y. Koga
Division of Oral Pathology and Bone Metabolism,
Department of Developmental and Reconstructive Medicine,
Nagasaki University Graduate School of Biomedical Sciences,
Nagasaki, Japan

Introduction

Lenz–Majewski syndrome (LMS) (OMIM 151050) is a rare sclerosing bone dysplasia, first described by Braham (1969) in 1969 and subsequently named Lenz–Majewski hyperostotic dwarfism (Lenz and Majewski 1974; Robinow et al. 1977). Only nine affected individuals have been reported to date, and all were sporadic (Braham 1969; Macpherson 1974; Kaye et al. 1974; Lenz and Majewski 1974; Robinow et al. 1977; Gorlin and Whitley 1983; Chrzanowska et al. 1989; Nishimura et al. 1997; Saraiva 2000; Wattanasirichaigoon et al. 2004). The skeletal changes include progressive hyperostosis of the craniofacial bones with delayed closure of the fontanelles, diaphyseal cortical thickening of the tubular bones, and brachymesophalangy with proximal symphalangism. In addition, affected individuals show moderate to severe mental retardation, severe growth failure, cutis laxa, enamel hypoplasia, choanal atresia, nasolacrimal duct obstruction, and webbed fingers and toes. The prognosis is

guarded. Most patients that have been reporteddied during childhood (Braham 1969; Macpherson 1974; Kaye et al. 1974; Majewski 2000). We report here on a Japanese boy whose manifestations can be considered to be a mild variant of LMS. Our experience raises the suspicion that the phenotypic range of LMS is broader than currently believed.

Clinical report

The patient was a 17-year-old Japanese boy born to nonconsanguineous healthy parents who were respectively 25 (mother) and 30 (father) years old at his birth. The family history was unremarkable. He was vaginally delivered at 40 weeks of gestation after an uneventful pregnancy. Apgar scores at 1 and 5 min were 8 and 10, respectively. Birth weight was 2300 g (–2.25 SD), length was 45 cm (–1.9 SD), and head circumference was 32.5 cm (–0.7 SD). Cutis laxa and prominent veins in the scalp and abdominal wall attracted medical attention in infancy, but a skin biopsy was not contributory. Psychomotor development was mildly retarded, with the infant showing head control at 6 months, walking alone at 20 months, and speaking meaning words at 24 months. Deciduous teeth were reported to have erupted at 2 years of age. The lack of eruptions of some permanent teeth in the upper jaw at 13 years of age was the basis for his referral to our hospital for further evaluation. His four maxillary permanent teeth of central and lateral incisors did not erupt. He had also a follicular cyst around the anterior teeth, necessitating surgical extirpation. Enamel dysplasia was histologically confirmed. He showed a distinctive, progeroid facial appearance with sparse hair, large auricles, maxillar hypoplasia, high-arched palate, and prognathism (Fig. 1a,

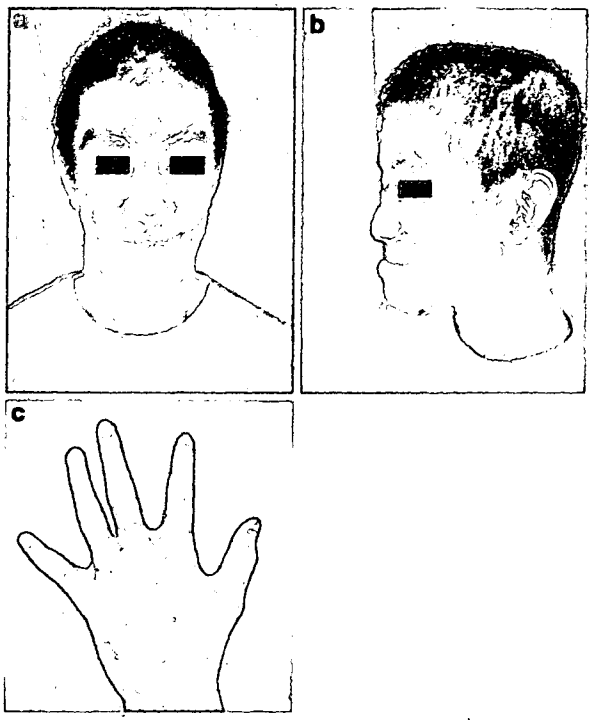

Fig. 1 Clinical photographs at 17 years of age. **a**, **b** A progeroid facial appearance with sparse hair, large auricles, and prognathism. **c** Interdigital webbing

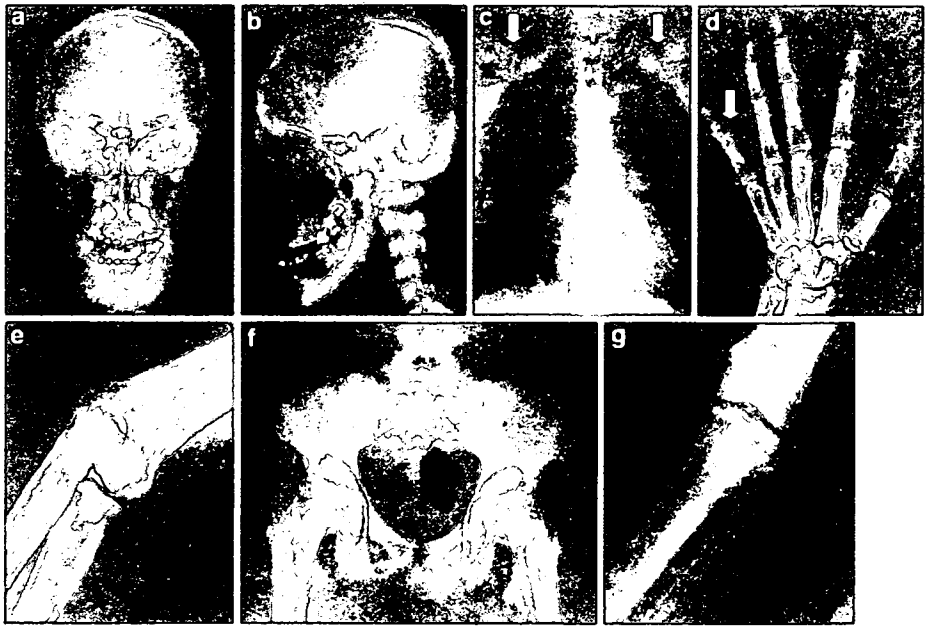

Fig. 2 Radiological findings at 17 years of age. **a**, **b** Hyperostosis of the calvaria, skull base and mandible. **c** Broad clavicles (*arrows*) and ribs, and sclerosis of metaphyseal equivalents of the spine. **d** Undermodeling of the short tubular bones and sclerosis of the carpal bones. **e** Metaepiphyseal sclerosis of the distal humerus, proximal ulna, and proximal radius. **f** Sclerosis of the sacrum, acetabulum, and proximal femur. **g** Sclerotic striations in the distal femur and proximal tibia

Table 1 Clinical and radiological findings of Lenz–Majewski syndrome (LMS)

Features	Typical LMS								Atypical LMS		Number of report (n = 10)
	Braham (1969); Macpherson (1974)	Lenz and Majewski (1974)	Kaye et al. (1974)	Robinow et al. (1977)	Gorlin and Whitley (1983)	Saraiva (2000)	Wattanasiri-chaigoon et al. (2004)	Chrzanowska et al.(1989)	Nishimura et al. (1997)	Our case	
Sex	Male	Female	Male	Male	Male	Female	Female	Male	Male	Male	
Gestational age	ND	Term	40 weeks	Term	Term	37 weeks	Term	Term	25 weeks	40 weeks	
Birth measurements											
Length (cm)	ND	45	ND	44.5	47	45	40	52	36	45	
Weight (g)	ND	2650	2300	2395	2800	3470	2100	2550	886	2300	
Head circumference (cm)	ND	34	ND	31.1	35	33	30	35	24	32.5	
Postnatal development											
Growth retardation	+	+	+	+	+	+	+	+	+	–	9/10
Mental retardation[a]	+	+	+	+	+	+	+	+	+	+	10/10
Emaciation	+	+	+	+	–	+	+	–	+	–	7/10
Physical features											
Delayed closure of fontanel[a]	+	+	+	+	+	+	+	ND	+	+	9/9
Dental enamel dysplasia[a]	+	+	+	+	+	+	ND	ND	+	+	8/8
Obstructed nasolacrimal ducts	+	+	ND	+	+	+	ND	ND	ND	–	5/6
Choanal atresia	+	+	ND	+	+	+	ND	ND	ND	–	5/6
Hyper extensible joints[a]	+	+	+	+	+	ND	+	+	ND	+	8/8
Proximal symphalangism	+	+	+	+	+	+	+	+	–	–	8/10
Interdigital webbing	+	+	+	+	+	+	+	+	–	+	9/10
Loose atrophic skin[a]	+	+	+	+	+	+	+	+	+	+	10/10
Prominent cutaneous veins[a]	+	+	+	+	+	+	+	ND	ND	+	8/8
Large floppy ears[a]	+	+	+	+	+	+	+	+	+	+	10/10
Radiographic features											
Progressive sclerosis of skull[a]	+	+	ND	+	+	+	+	+	+	+	9/9
Broad clavicles and ribs	+	+	ND	+	+	+	+	–	+	+	8/9
Short middle phalanges	+	+	+	+	+	ND	+	+	–	+	8/9
Diaphyseal undermodeling[a]	+	+	ND	+	+	+	ND	ND	+	+	7/7
Diaphyseal hyperostosis	+	+	ND	+	+	ND	+	+	–	–	6/8
Metaphyseal and epiphyseal radiolucency[a]	+	+	ND	+	+	ND	ND	ND	+	–	5/6

ND, Not described; +, present; –, absent

[a] Clinical features common to all reported cases

b). He had inter-digital webbing (Fig. 1c) and mild cubitus valgus. The skin was wrinkled and loose, and prominent veins were noted in the abdominal wall. He had mild mental retardation with a total intelligence quotient of 60. Radiological examination showed cranial hyperostosis, particularly of the skull base, a sclerotic, thick mandible, broad clavicles and ribs, and diaphyseal undermodeling of the tubular bones. Diaphyseal hyperostosis was not evident, while epimetaphyseal sclerosis or longitudinal sclerotic striation was found in the long bones. Metaphyseal equivalents of the axial skeleton showed dense sclerosis (Fig. 2a–g). Bone scintigraphy showed an increased accumulation of radiopharmaceuticals, corresponding with sclerotic regions on the roentgenograms. During follow-up to 17 years of age, he showed a stable clinical course. At 17 years of age, he had a muscular build, a height of 164.5 cm (–1.0 SD) and a head circumference of 54 cm (–1.3 SD) and weighed 56.2 kg (–0.54 SD). He underwent a surgical correction for severe anterior occlusion with prognathism. Mutation analyses for the transforming growth factor-beta1 gene (*TGFB1*) and the LDL receptor-related protein 5 gene (*LRP5*) yielded normal findings.

Discussion

We describe a boy with a disorder that is classifiable into a group of sclerosing bone dysplasias. The disorder was radiologically characterized by cranial hyperostosis, metaepiphyseal sclerosis, and diaphyseal undermodeling. In addition, it was uniquely associated with cutis laxa, enamel dysplasia, and mental retardation. According to the 'Nosology and Classification of Genetic Skeletal Disorders: 2006 revision' (Superti-Furga and Unger 2007), sclerosing bone dysplasias are subclassified into three groups: (1) neonatal osteosclerotic dysplasia group, (2) increased bone density group (without modification of bone shape), and (3) increased bone density group with metaphyseal and/or diaphyseal involvement. A few disorders in the third group, such as Camurati–Engelmann disease, craniometaphyseal dysplasia, craniodiaphyseal dysplasia, and endosteal hyperostosis, share some radiological features with the present disorder. However, the unique constellation of skeletal, skin, dental, and mental abnormalities in the present disorder excludes the possibility of these disorders. In fact, molecular analyses for *TGFB1* (the gene of Camurati–Engelmann disease) and *LRP5* (the gene of endosteal hyperostosis, Worth type) were negative.

In the differential diagnosis, LMS deserves to be discussed. The disorder is characterized by craniodiaphyseal hyperostosis and brachymesophalangy with proximal symphalangism. It is complicated by mental retardation, somatic growth failure, cutis laxa, enamel hypoplasia, and webbed fingers and toes. The manifestations of previously reported LMS patients, LMS-like patients, and the present patient are summarized in Table 1. Most findings in LMS were shared by the present disorder. However, the differences include the absence of somatic growth failure and brachymesophalangy with proximal symphalangism in the present patient. LMS patients typically exhibit diaphyseal hyperostosis and metaepiphyseal radiolucency, while the present patient had only diaphyseal undermodeling and showed metaepiphyseal sclerosis. However, the degree of diaphyseal hyperostosis is described to vary considerably among LMS patients, and some patients with metaepiphyseal sclerosis are reported in the literature (Chrzanowska et al. 1989; Spranger et al. 2002). Thus, it is tempting to assume that the present disorder may fall at the mildest end in the phenotypic continuum of LMS, suggesting that the clinical spectrum of the disorder may be broader than currently thought.

References

Braham RL (1969) Multiple congenital abnormalities with diaphyseal dysplasia (Camurati–Engelmann's syndrome). Oral Surg 27:20–26

Chrzanowska KH, Fryns JP, Krajewska M, Van den Berghe H, Wisniewski L (1989) Skeletal dysplasia syndrome with progeroid appearance, characteristic facial and limb anomalies, multiple synostoses, and distinct skeletal changes: a variant example of the Lenz–Majewski syndrome. Am J Med Genet 32:470–474

Gorlin RJ, Whitley CB (1983) Lenz–Majewski syndrome. Radiology 149:129–131

Kaye CI, Fisher DE, Esterly NB (1974) Cutis laxa, skeletal anomalies, and ambiguous genitalia. Am J Dis Child 127:115–117

Lenz W, Majewski F (1974) A generalized disorder of the connective tissues with progeria, choanal atresia, symphalangism, hypoplasia of dentine and craniodiaphysial hypostosis. Birth Defects Orig Arctic Ser 10:133–136

Macpherson RI (1974) Craniaodiaphyseal dysplasia, a disease or group of diseases? J Can Assoc Radiol 25:22–33

Majewski F (2000) Lenz–Majewski hyperostotic dwarfism: reexamination of the original patient. Am J Med Genet 93:335–338

Nishimura G, Harigaya A, Kuwashima M, Kuwashima S (1997) Craniotubular dysplasia with severe postnatal growth retardation, mental retardation, ectodermal dysplasia, and loose skin: Lenz–Majewski-like syndrome. Am J Med Genet 71:87–92

Robinow M, Johanson AJ, Smith TH (1977) The Lenz–Majewski hyperostotic dwarfism. J Pediatr 91:417–421

Saraiva JM (2000) Dysgenesis of corpus callosum in Lenz–Majewski hyperostotic dwarfism. Am J Med Genet 91:200–202

Superti-Furga A, Unger S (2007) Nosology and classification of genetic skeletal disorders: 2006 revision. Am J Med Genet 143A:1–18

Spranger JW, Brill PW, Poznanski A (2002) Bone dysplasias: an atlas of genetic disorders of skeletal development, 2nd edn. Oxford University Press, Oxford

Wattanasirichaigoon D, Visudtibhan A, Jaovisidha S, Laothamatas J, Chunharas A (2004) Expanding the phenotypic spectrum of Lenz–Majewski syndrome: facial palsy, cleft palate and hydrocephalus. Clin Dysmorph 13:137–142

REPORT

CHMP4B, a Novel Gene for Autosomal Dominant Cataracts Linked to Chromosome 20q

Alan Shiels, Thomas M. Bennett, Harry L. S. Knopf, Koki Yamada, Koh-ichiro Yoshiura, Norio Niikawa, Soomin Shim, and Phyllis I. Hanson

Cataracts are a clinically diverse and genetically heterogeneous disorder of the crystalline lens and a leading cause of visual impairment. Here we report linkage of autosomal dominant "progressive childhood posterior subcapsular" cataracts segregating in a white family to short tandem repeat (STR) markers *D20S847* (LOD score [*Z*] 5.50 at recombination fraction [θ] 0.0) and *D20S195* ($Z = 3.65$ at $\theta = 0.0$) on 20q, and identify a refined disease interval (*rs2057262*–(3.8 Mb)–*rs1291139*) by use of single-nucleotide polymorphism (SNP) markers. Mutation profiling of positional-candidate genes detected a heterozygous transversion (c.386A→T) in exon 3 of the gene for chromatin modifying protein-4B (*CHMP4B*) that was predicted to result in the nonconservative substitution of a valine residue for a phylogenetically conserved aspartic acid residue at codon 129 (p.D129V). In addition, we have detected a heterozygous transition (c.481G→A) in exon 3 of *CHMP4B* cosegregating with autosomal dominant posterior polar cataracts in a Japanese family that was predicted to result in the missense substitution of lysine for a conserved glutamic acid residue at codon 161 (p.E161K). Transfection studies of cultured cells revealed that a truncated form of recombinant D129V-CHMP4B had a different subcellular distribution than wild type and an increased capacity to inhibit release of virus-like particles from the cell surface, consistent with deleterious gain-of-function effects. These data provide the first evidence that *CHMP4B*, which encodes a key component of the endosome sorting complex required for the transport-III (ESCRT-III) system of mammalian cells, plays a vital role in the maintenance of lens transparency.

Hereditary forms of cataracts are usually diagnosed at birth (congenital), during infancy, or during childhood and are clinically important as a cause of impaired form vision development.[1] In addition to being found in >50 genetic syndromes involving other ocular defects (e.g., microphthalmia [MIM 212550]) and systemic abnormalities (e.g., galactokinase deficiency [MIM 230200]), cataracts may be inherited as an isolated lens phenotype, most frequently by autosomal dominant transmission.[2] So far, genetic linkage studies of >60 families worldwide have mapped at least 25 independent loci for clinically diverse forms of nonsyndromic cataracts on 15 human chromosomes, involving some 17 lens-abundant genes.[2] The majority of associated mutations have been identified in 10 crystallin genes (*CRYAA* [MIM 123580], *CRYAB* [MIM 123590], *CRYBB1* [MIM 600929], *CRYBB2* [MIM 123620], *CRYBB3* [MIM 123630], *CRYBA1* [MIM 123610], *CRYBA4* [MIM 123631], *CRYGC* [MIM 123680], *CRYGD* [MIM 123690], and *CRYGS* [MIM 123730]),[3–11] which encode the major "refractive" proteins of the lens. The remaining mutations have been identified in seven functionally diverse genes, including those coding for gap-junction connexin proteins (*GJA3* [MIM 121015], *GJA8* [MIM 600897]),[12,13] a heat-shock transcription factor (*HSF4* [MIM 602438]),[14] an aquaporin water channel (*MIP* [MIM 154050])[15] a claudin-like cell-junction protein (*LIM2* [MIM 154045]),[16] and intermediate-filament-like cytoskeletal proteins (*BFSP1* [MIM 603307], *BFSP2* [MIM 603212]).[17,18] In addition to the known genes, at least 10 novel genes for autosomal dominant or recessive forms of nonsyndromic cataracts remain to be identified at loci on chromosomes 1 (CCV [MIM 115665], CTPP1 [MIM 116600]), 2 (PCC [MIM 601286], CCNP [MIM 607304, MIM 115800]), 3 (CATC2 [MIM 610019]), 9 (CAAR [MIM 605749]), 15 (CCSSO [MIM 605728]), 17 (CTAA2 [MIM 601202], CCA1 [MIM 115660]), 19 (CATCN1 [MIM 609376]), and 20 (CPP3 [MIM 605387]).[19–32] Here we have fine-mapped a locus for autosomal dominant cataracts on chromosome 20q and, subsequently, have identified underlying missense mutations in the gene for chromatin modifying protein-4B (*CHMP4B* [MIM 610897]), also known as charged multivesicular body protein-4B, which has not previously been associated with human disease.

Linkage studies.—We investigated a six-generation white family from the United States (family Sk) segregating autosomal dominant progressive childhood posterior subcapsular cataracts (PCPSC) in the absence of other ocular or systemic abnormalities (fig. 1*A*). Ophthalmic records indicated that the cataracts presented in both eyes as disc-shaped posterior subcapsular opacities, progressing with age to affect the nucleus and anterior subcapsular regions of the lens (fig. 1*B*). The age at diagnosis varied from 4 to

From the Departments of Ophthalmology and Visual Sciences (A.S.; T.M.B.; H.L.S.K.), Genetics (A.S.), and Cell Biology and Physiology (S.S.; P.I.H.), Washington University School of Medicine, St. Louis, MO; and the Departments of Ophthalmology and Visual Sciences (K.Y.), and Human Genetics (K-i.Y.; N.N), Nagasaki University Graduate School of Biomedical Sciences, Nagasaki, Japan

Received March 9, 2007; accepted for publication May 9, 2007; electronically published July 27, 2007.

Address for correspondence and reprints: Dr. Alan Shiels, Department of Ophthalmology and Visual Sciences, Campus Box 8096, Washington University School of Medicine, 660 South Euclid Avenue, St. Louis, MO 63110. E-mail: shiels@vision.wustl.edu

Am. J. Hum. Genet. 2007;81:596–606. 0002-9297/2007/8103-0017$15.00
DOI: 10.1086/519980

20 years, and the age at surgery ranged from 4 to 40 years. Postsurgical corrected visual acuity varied from 20/20 to 20/200 in the better eye. Blood samples were obtained from 27 family members, and leukocyte genomic DNA was purified and quantified using standard techniques (Qiagen). Ethical approval for this study was obtained from the Washington University Human Research Protection Office, and written informed consent was provided by all participants prior to enrollment, in accordance with the tenets of the Declaration of Helsinki.

For linkage analysis, 15 affected individuals, 8 unaffected individuals, and 4 spouses from family Sk were genotyped using STR markers from the combined Généthon, Marshfield, and deCODE genetic linkage maps (National Center for Biotechnology Information [NCBI]), as described elsewhere.[33] Following exclusion of linkage to known loci for autosomal dominant cataracts on chromosomes 1–3, 10–13, 15–17, 19, 21, and 22 (table 1), we obtained significant evidence of linkage (table 2) for markers *D20S847* ($Z = 5.50$ and $\theta = 0$), *D20S195* ($Z = 3.65$ and $\theta = 0$), and *D20S870* ($Z = 3.11$ and $\theta = 0$).

Haplotype analysis detected seven recombinant individuals within the Sk pedigree (fig. 1*A*). First, two affected females, VI:4 and VI:6, were obligate recombinants, proximally at *D20S885* and distally at *D20S855*, respectively. Second, three affected females (IV:1, IV:4, and V:3) and one affected male (VI:1) were obligate recombinants distally at *D20S834*. Third, one affected female (V:3) and her affected son (VI:1) were obligate recombinants proximally at *D20S837*. However, with the exception of individual V:5 (see below), no further recombinant individuals were detected at four other intervening STR markers, suggesting that the cataract locus lay in the physical interval, *D20S837*–(4.7 Mb)–*D20S834*.

At the time of our study, individual V:5 was 17 years of age and phenotypically unaffected; however, he inherited the complete disease haplotype (fig. 1*A*), suggesting that he was either nonpenetrant or presymptomatic for cataracts. The two-point LOD scores shown in table 2 were calculated with the assumption of unaffected status for individual V:5 and 95% penetrance in family Sk; however, even when 100% penetrance was assumed, we still retained significant evidence of linkage proximally at *D20S195* ($Z_{max} = 4.31$ at $\theta_{max} = 0.04$) and distally at *D20S847* ($Z_{max} = 5.08$ at $\theta_{max} = 0.04$). Conversely, if individual V:5 developed cataracts later in life, perhaps extending the age-at-onset range in family Sk, and was included with the assumption of preaffected status and 100% penetrance, we would obtain enhanced evidence for linkage (*D20S195*, $Z_{max} = 5.12$ at $\theta_{max} = 0.0$; *D20S847*, $Z_{max} = 6.97$ at $\theta_{max} = 0.0$). However, regardless of whether individual V:5 was included or excluded, we found no evidence of linkage at other candidate genes or loci for autosomal dominant cataracts (table 1).

To further refine the disease interval, we genotyped family Sk with biallelic SNP markers (NCBI) located within the STR interval using conventional dye-terminator cycle-sequencing chemistry (Applied Biosystems). Critical affected individuals IV:1, IV:4, and V:3 were also found to be recombinant at SNP marker *rs1291139* (A/T), which lies ~0.5 Mb centromeric to *D20S834*. Similarly, critical affected individuals V:3, and VI:1 were also recombinant at marker *rs2057262* (A/C) located ~0.4 Mb telomeric to *D20S837* (fig. 1*A*). However, individual V:5 excepted, no further recombination events were detected at intervening SNP markers, indicating that the cataract locus lay in the reduced (~0.9 Mb) physical interval, *rs2057262*–(3.8 Mb)–*rs1291139* (fig. 1*C*).

Mutation analysis.—The refined SNP interval contained ~80 positional-candidate genes, none of which were obvious functional candidates for cataracts in family Sk (NCBI Map Viewer). We prioritized genes for mutation analysis of exons and intron boundaries (splice sites) on the basis of three main criteria.

1. NCBI reference sequence status, with those genes designated "reviewed" or "provisional" selected over those designated "model" or "pseudogene."
2. Evidence of expression in (fetal) eye, from the UniGene EST database.
3. Number of exons or amplicons required for coverage of the coding region, starting with smaller genes first.

Resequencing analysis of individuals IV:5, V:6, V:10, and VI:6 from the Sk pedigree (fig. 1*A*) excluded the presence of coding or splice-site mutations in eight genes (data not shown), including *EPB41L1* (MIM 602879), *E2F1* (MIM 189971), *ZNF341, PXMP4, ITGB4BP* (MIM 602912), *APBA2BP, SCAND1* (MIM 610416), and *DYNLRB1* (MIM 607167). However, resequencing of a 5-exon gene symbolized *CHMP4B* (GeneID: 128866) identified a heterozygous c.386A→T transversion in exon 3 that was not present in wild type (fig. 2*B*). This single-nucleotide change did not result in the gain or loss of a convenient restriction site; therefore, we designed allele-specific (A/T) PCR analysis to confirm that the mutant "T" allele cosegregated with affected but not unaffected members of family Sk, with the exception of individual V:5 (fig. 2*C*). Furthermore, when we tested the c.386A→T transversion as a biallelic marker, with a notional allelic frequency of 1%, in a two-point LOD score analysis of the cataract locus (table 2) we obtained further compelling evidence of linkage ($Z = 6.52$ at $\theta = 0$). In addition, we confirmed that the c.386A→T transversion was not listed in the NCBI SNP database (dbSNP), and we excluded it as a SNP in a panel of 192 normal, unrelated individuals (i.e., 384 chromosomes), using the allele-specific PCR analysis described in fig. 2*C* (data not shown). Although it is possible that an undetected mutation lay elsewhere within the disease-haplotype interval (3.8 Mb), our genotype data strongly suggested that the c.386A→T transversion in exon 3 of *CHMP4B* represented a causative mutation rather than a benign SNP in linkage disequilibrium with the cataract phenotype.

To verify that the c.386A→T transversion in *CHMP4B*

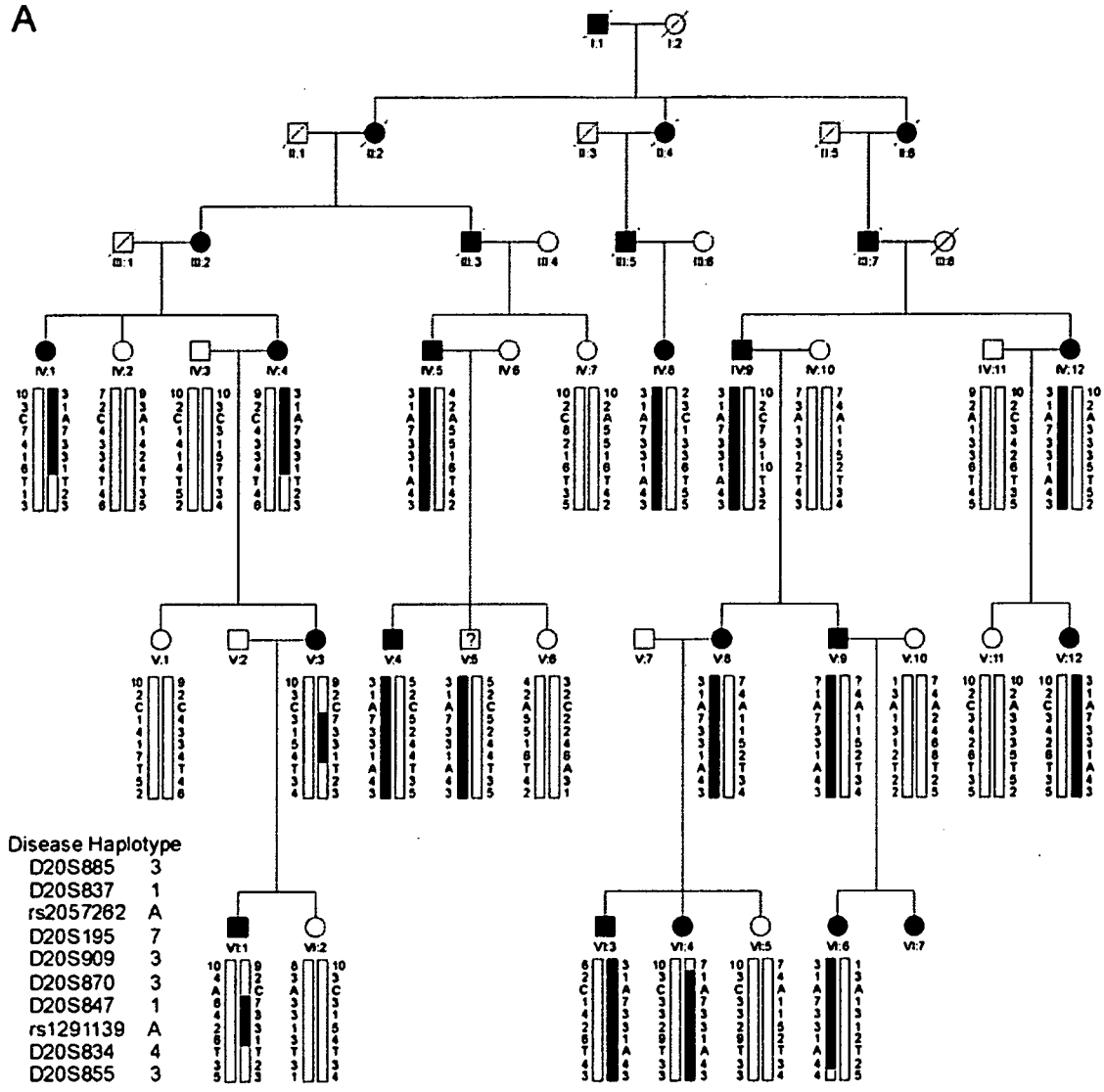
A
Disease Haplotype
D20S885 3
D20S837 1
rs2057262 A
D20S195 7
D20S909 3
D20S870 3
D20S847 1
rs1291139 A
D20S834 4
D20S855 3

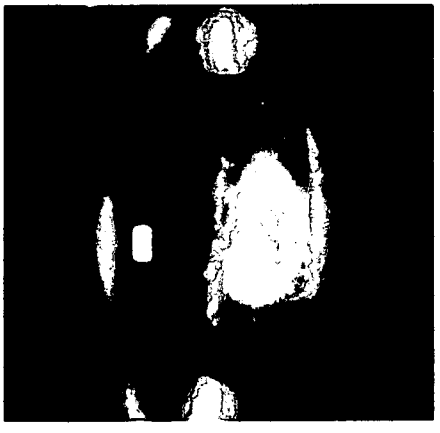
B

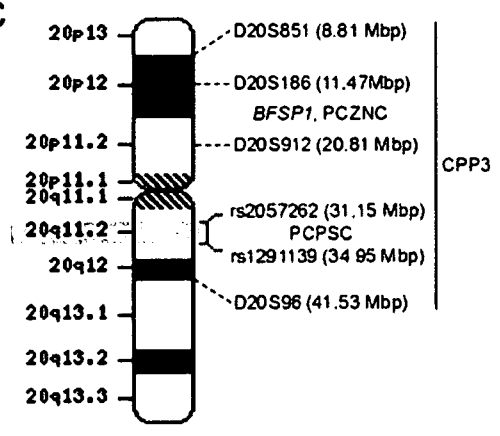
C
20p13
20p12
20p11.2
20p11.1
20q11.1
20q11.2
20q12
20q13.1
20q13.2
20q13.3
D20S851 (8.81 Mbp)
D20S186 (11.47Mbp)
BFSP1, PCZNC
D20S912 (20.81 Mbp)
rs2057262 (31.15 Mbp)
PCPSC
rs1291139 (34.95 Mbp)
D20S96 (41.53 Mbp)
CPP3

was present at the RNA transcript level in family Sk, we performed allele-specific RT-PCR analysis of peripheral blood leukocytes (PBLs), which have been shown to express *CHMP4B*.[35] PCR primers (table 3) were designed to amplify the entire coding region of *CHMP4B* (codons 1–224) in the presence of a nested mutant (T allele) primer to detect heterozygosity in three consenting relatives, including individual V:5 (fig. 3*A*). The affected father (IV:5) and his son (V:5) were heterozygous for the wild-type (A allele) and mutant (T allele) transcripts, whereas his unaffected daughter (V:6) was homozygous for the wild-type (A allele) transcript. To gain a more accurate comparison of wild-type versus mutant CHMP4B transcript levels in PBL RNA, we then performed quantitative (q)RT-PCR with SYBR Green-1 in real time (fig. 3*B*), using a sense anchor primer paired with either a mutant (T allele) or wild-type (A allele) primer (table 3). When standardized against transcript levels for the midabundance ribosomal protein-L19 (RPL19), the ratio of wild-type to mutant CHMP4B transcripts was estimated to be 60(A):40(T), suggesting decreased expression and/or increased turnover of the mutant transcript in affected individuals. Overall, the transcript and genotype data are consistent for these individuals (fig. 1*A* and fig. 3*A*) and support the view that the clinically unaffected son (V:5) is either presymptomatic or nonpenetrant for the cataract phenotype. Moreover, the ability to amplify the intact coding region of CHMP4B transcripts from affected individuals was consistent with correct mRNA splicing, suggesting that the c.386A→T transversion, which is located near the beginning of exon 3, did not activate a cryptic splice site.[36] Finally, we also confirmed that the intact coding region of CHMP4B transcripts could be amplified from human and mouse post mortem lenses (fig. 3*C*), consistent with a functional role for CHMP4B in lens biology.

CHMP4B is cytogenetically distinct from *BFSP1* and an interval on 20p (fig. 1*C*) that was linked recently with autosomal dominant progressive congenital zonular nuclear cataract (PCZNC) segregating in a Chinese family.[32] However, *CHMP4B* is located within a much larger region spanning 20p12–20q12 that was previously linked with autosomal dominant posterior polar cataract (CPP3 [MIM 605387]) segregating in a Japanese family.[31] Like the cataracts in family Sk, CPP3 was characterized by a juvenile onset and progressive disc-shaped posterior subcapsular opacities along with some cortical opacification.[37] To investigate the possibility of allelism, we performed a similar mutation screen of *CHMP4B* in the CPP3 family and identified a heterozygous c.481G→A transition in exon 3 that was not present in wild type (fig. 4*A* and 4*B*) or in the SNP database. This single-nucleotide change removed an adjacent *Mnl*1 restriction enzyme-site, and restriction fragment length analysis confirmed that the heterozygous A allele cosegregated with affected members of the CPP3 family but was not present in unaffected relatives or our control panel (fig. 4*C* and data not shown). The identification of a second coding nucleotide change in a geographically and ethnically distinct family provided strong supporting evidence for *CHMP4B* as the causative gene for cataracts linked to 20q. In addition, the locus for lens opacity-4 (*Lop4*)[38] has been linked to a region of murine chromosome 2 that is syntenic with human 20q11.2 raising the possibility of a mouse model for the cataracts described here.

CHMP4B encodes a highly charged helical protein (~25 kDa) with N-terminal basic and C-terminal acidic halves (fig. 5*B*). The c.386A→T transversion in exon 3 occurred at the second base of codon 129 (GAT→GTT), and is predicted to result in the missense substitution of aspartic acid to valine (p.D129V) at the level of translation. Similarly, the c.481G→A transition occurred at the first base of codon 161 (GAG→AAG) of exon 3, and is predicted to translate as a missense substitution of glutamic acid to lysine (p.E161K). Cross-species alignment of the amino acid sequences for CHMP4B present in the Entrez Protein database, performed by means of ClustalW, revealed that p.D129 and p.E161 are phylogenetically conserved from yeast to man (fig. 5*C*). Moreover, the predicted p.D129V and p.E161K substitutions represented nonconservative amino acid changes, with the acidic side-group ($-CH_2COOH$) of aspartic acid replaced by the neutral, hydrophobic side-group ($-CH-C_2H_6$) of valine, and the acidic side-group ($-C_2H_4COOH$) of glutamic acid replaced by the basic side-group ($-C_4H_8NH_2$) of lysine, respectively, suggestive of functional consequences.

Functional expression studies.—Eleven CHMP genes have been identified in the human genome and, on the basis of phylogenetic analyses, have been divided into seven subfamilies, some with multiple members.[39,40] CHMP4B is one of three human orthologs of yeast Snf7/Vps32 (sucrose non-fermenting-7 or vacuolar protein sorting-32), which functions in protein sorting and transport in the endosome-lysosome pathway.[39] In the current model, CHMP4B is a core subunit of the endosomal-sorting com-

Figure 1. Autosomal dominant PCPSC in a six-generation family (Sk). *A*, Pedigree and haplotype analysis showing segregation of eight STR markers and two SNP markers on 20q, listed in descending order from the centromere. Squares and circles denote males and females, respectively. Filled symbols and bars denote affected status and haplotypes, respectively. Individual V:5 is marked with a question mark (?) to denote unknown status. Pedigree and haplotype data were managed using Cyrillic 2.1 software (FamilyGenetix). *B*, Slit-lamp image of lens from affected female V:12 (age 40 years) showing posterior subcapsular, nuclear, and anterior subcapsular opacities. *C*, Ideogram of chromosome 20, comparing the cytogenetic location of SNP markers defining the PCPSC locus in this study (*red*) with those of STR markers defining loci for CPP3 and PCZNC.[31,32]

Table 1. Two-point LOD scores (Z) Showing Exclusion of Linkage between the Autosomal Dominant Cataract Locus and STR Markers near Candidate Genes or Loci on Chromosomes Other Than 20

Marker	Z^*	θ	Chromosome	Gene/Locus
D1S243	−2.77	.10	1p36	CCV, CPP1
D1S214	−2.93	.10		
D1S2748	−2.14	.20	1p32	*FOXE3*[MIM 601094]
D1S305	−2.01	.20	1q21	*GJA8*
D2S2333	−2.35	.20	2p12	CCNP
D2S128	−3.19	.05	2q32-q36	*CRYGC, CRYGD, CRYBA2*
D2S2248	−2.75	.20		
D3S1768	−∞	.00	3p21.1-p21.3	CATC2
D3S3564	−2.34	.05		
D3S1292	−1.76	.05	3q22.1	*BFSP2*
D3S3686	−4.04	.10	3q27.2	*CRYGS*
D5S2014	−2.05	.05	5q33.1	*SPARC* [MIM 182120]
D6S1710	−2.37	.05	6q12	*GLULD1*
D9S303	−1.31	.05	9q21.31	CAAR
D9S1120	−1.28	.05		
D10S566	−2.94	.10	10q24-q25	*PITX3*[MIM 602669]
D10S1697	−3.01	.10		
D11S4154	−2.63	.05	11p13	*PAX6* [MIM 607108]
D11S4192	−2.55	.10	11q23.1	*CRYAB*
D11S1347	−3.28	.05		
D12S368	−1.94	.10	12q13.3	*MIP*
D13S175	−2.34	.05	13q11	*GJA3*
D14S1047	−2.12	.05	14q24.3	*CHX10*[MIM 142993]
D15S209	−3.14	.05	15q21-q22	CCSS0
D15S1036	−2.41	.20		
D16S412	−2.51	.10	16p12.3	*CRYM*[MIM 123740]
D16S3095	−2.99	.10	16q22.1	*HSF4*
D17S1840	−2.45	.05	17p13	CTAA2
D17S796	−2.13	.10		
D17S799	−1.79	.05	17q11.2	*CRYBA1*
D17S798	−1.18	.05		
D17S785	−2.14	.10	17q24	*GALK1*[MIM 604313]
D17S802	−1.91	.05	17q24	CCA1
D17S784	−2.67	.10		
D19S412	−2.41	.15	19q13	*LIM2*
D20S112	2.58	.08	20p11.23	*BFSP1*
D20S885	2.71	.10	20p12-20q12	CPP3
D20S847	5.08	.04		
D21S1259	−2.78	.10	21q22.3	*CRYAA*
D21S1885	−.81	.00		
D22S1154	−2.20	.15	22q11.23-q21.1	*CRYBA4, CRYBB1-4*

* A gene frequency of 0.0001 and a penetrance of 100% were assumed for the disease locus.

plex required for transport-III (ESCRT-III), which facilitates the biogenesis of multivesicular bodies (MVBs).[39] The only CHMP gene so far implicated in human disease is *CHMP2B* (yeast ortholog Vps2/Did4 [MIM 609512]), which has been reported to harbor mutations infrequently associated with frontotemporal dementia (FTD [MIM 600795]) and amyotropic lateral sclerosis (ALS [MIM 609512]).[41–43]

CHMP4B is found diffusely throughout the cytoplasm and/or in association with endosome-like compartments when expressed in cultured mammalian cells.[44,45] To determine the effect of the p.D129V substitution on the subcellular distribution of CHMP4B, we transfected African green monkey kidney (COS-7) cells with expression plasmids[46] encoding either wild-type or mutant forms of CHMP4B tagged at the N-terminus with the FLAG epitope. Immunofluorescence microscopy with FLAG antibody revealed that full-length wild-type (FLAG-CHMP4B) and mutant protein (FLAG-D129V-CHMP4B) were diffusely distributed (fig. 6*A* and 6*B*). At higher expression levels, both were associated with endosome-like compartments (data not shown). Overall, there were no notable differences in the subcellular localization of wild type and

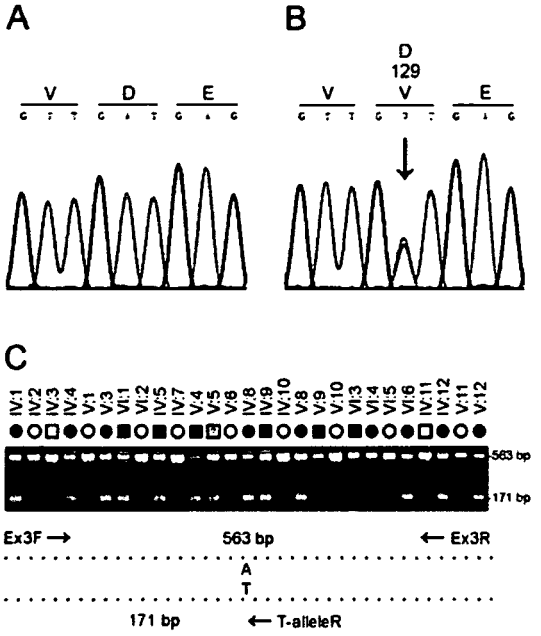

Figure 2. Mutation analysis of *CHMP4B* in family Sk. *A*, Sequence trace of the wild-type allele, showing translation of aspartic-acid (D) at codon 129 (GAT). *B*, Sequence trace of the mutant allele, showing the heterozygous c.386A→T transversion (denoted as W by the International Union of Pure and Applied Chemistry [IUPAC] code) that is predicted to result in the missense substitution of valine (GTT) for aspartate at codon 129 (p.D129V). Exons and flanking intron regions were amplified with gene-specific primers (M13-tailed) by use of the AmpliTaq PCR Master Mix in a GeneAmp 9700 thermal-cycler (Applied Biosystems). Resulting amplicons were purified using the QIAquick gel-extraction kit (Qiagen) and then direct sequenced in both directions with M13-primers and the BigDye Terminator (v.3.1) cycle sequencing kit on a 3130xl genetic analyzer running SeqScape mutation-profiling software (Applied Biosystems). *C*, Allele-specific PCR analysis using the three primers (table 3) indicated by arrows in the schematic diagram; exon 3 was amplified as above with the sense (anchor) primer located in intron 2 (Ex3F), the anti-sense primer located in intron 3 (Ex3R), and the nested mutant primer specific for the T allele in codon 129 (T-alleleR). PCR products were visualized (302 nm) on 2% agarose gels stained with ethidium bromide (EtBr). Note that only affected members of family Sk are heterozygous for the T allele (171 bp), with the exception of individual V:5, who is believed to be presymptomatic or nonpenetrant for cataracts.

Table 2. Two-Point LOD Scores (Z) for Linkage between the Cataract Locus and Markers on Chromosome 20q Listed in Physical Order (Mb) from the Short-Arm Telomere (p-tel)

Marker	Distance from p-tel		Z^a at θ =							
	cM	Mb	.00	.05	.10	.20	.30	.40	Z_{max}	θ_{max}
D20S885	39.9	17.91	−7.79	2.51	2.72	2.35	1.60	.74	2.72	.10
D20S111	49.2	29.94	−2.82	1.14	1.17	.91	.54	.19	1.18	.08
D20S837	50.7	30.73	−.81	4.15	3.98	3.18	2.14	1.01	4.15	.05
rs2057262		31.15	−4.03	−.02	.14	.16	.09	.03	.17	.15
D20S195	50.2	31.29	3.65	4.17	3.88	2.96	1.90	.87	4.20	.03
CHMP4B (A>T)		31.90	6.24	5.87	5.37	4.19	2.82	1.36	6.24	.00
D20S909	50.7	33.92	1.89	1.88	1.72	1.25	.73	.33	1.91	.02
D20S896	50.2	34.16	2.88	2.60	2.30	1.68	1.05	.46	2.88	.00
D20S870	50.7	34.16	3.11	2.93	2.63	1.94	1.23	.59	3.11	.00
D20S847	50.2	34.32	5.50	5.18	4.72	3.60	2.33	1.05	5.50	.00
rs1291139		34.95	−1.85	.99	1.10	.96	.66	.30	1.10	.11
D20S834	50.7	35.43	−1.08	2.07	1.91	1.30	.65	.19	2.07	.05
D20S607	54.9	38.23	−1.61	1.85	2.02	1.81	1.30	.66	2.03	.11
D20S855	56.0	39.08	−.29	3.26	3.19	2.58	1.71	.77	3.27	.06

NOTE.—STR marker allele frequencies used for linkage analysis were those calculated by Généthon/Marshfield/deCODE. A gene frequency of .0001 and a penetrance of 95% were assumed for the disease locus.

[a] Z values were calculated using the MLINK subprogram from the LINKAGE (5.1) package of programs.[34]

p.D129V mutant protein. In contrast, similar expression studies of a splicing mutation in *CHMP2B* underlying FTD, which resulted in truncation (36 amino acids) and miscoding (29 amino acids) at the C-terminus of the full-length protein (residues 1–213), has been associated with redistribution of CHMP2B and the formation of dysmorphic organelles of the late endosomal pathway.[41]

The p.D129V missense substitution was predicted to be located centrally in CHMP4B and to result in the net loss of a negatively charged residue (fig. 5*B*). Domain expression studies have revealed that the N-terminal half of CHMP4A (MIM 610051), an isoform of CHMP4B, is responsible for self-association into polymers and binding to membrane phospholipids.[46] To better appreciate the effects of the p.D129V substitution, we compared the subcellular localization of wild-type and mutant N-terminal fragments of CHMP4B (residues 1–150) comparable to those previously studied.[46,47] As expected, the distribution of the truncated wild-type fragment (FLAG-CHMP4B$_{1-150}$) differed from that of the full-length wild-type protein; the former appeared to be in large polymers and sometimes associated with vacuolar structures (fig. 6*C*), whereas the latter was diffuse (fig. 6*A*). Similarly, the truncated mutant fragment (FLAG-D129V-CHMP4B$_{1-150}$) differed from the full-length mutant protein; the former was concentrated on a punctate perinuclear structure (fig. 6*D*), and the latter was again diffuse (fig. 6*B*). Consistently, however, the truncated mutant fragment (fig. 6*D*) displayed a different subcellular distribution pattern from that of the truncated wild-type fragment (fig. 6*C*).

In addition to MVB formation, CHMP4B is thought to participate in the budding of a number of RNA viruses, including human immunodeficiency virus type-1 (HIV-1), from the surface of infected cells.[45] To further investigate the effect of the p.D129V substitution on CHMP4B activity in a functional assay, we compared the effect of expressing wild-type and mutant protein on release of HIV-1 virus-like-particles (VLPs). To monitor VLP production, human embryonic kidney (HEK 293T) cells were cotransfected with a plasmid encoding the HIV-1 Gag polyprotein (Pr55) and a plasmid encoding wild-type or mutant CHMP4B. HIV-1 Gag forms VLPs in the absence of other viral proteins,[48] and expression of Gag and CHMP4B

Table 3. PCR Primers for Mutation Screening and Transcript Analysis of *CHMP4B*

Primer	Location	Strand	Sequence (5′→3′)[a]
Ex1F	Exon 1	Sense	gtagtcagtggcgcgttg
Ex1R	Intron 1	Antisense	aggcgagtctgatgaaggtg
Ex2F	Intron 1	Sense	cactagaacctcaccctgtgc
Ex2R	Intron 2	Antisense	aaacaaactcaggtgctcgaa
Ex3F	Intron 2	Sense	tcacagggagtcattgcaggg
Ex3R	Intron 3	Antisense	cccaccctggaaaggtgcag
Ex3R2	Intron 3	Antisense	agggacagcctcagggtatcattt
Ex4F	Intron 3	Sense	cacagggtctggaacctggaa
Ex4R	Intron 4	Antisense	tgggcaagctcaggacacaga
Ex5F1	Intron 4	Sense	aacatgttgaacgcaccagtc
Ex5R1	Exon 5	Antisense	AGGTCATTTCAACTGCAACCA
Ex5F2	Exon 5	Sense	CGCTGACTCCACTGCTGAATCC
Ex5R2	Exon 5	Antisense	ctggaaagggtcagctcccg
StartF	Exon 1	Sense	caccATGTCGGTGTTCGGGAAGCT
EndR	Exon 5	Antisense	CATGGATCCAGCCCAGTTCTCCAA
A-alleleR	Exon 3	Antisense	CAGCAATGTCCTGCATTAACTCAT
T-alleleR	Exon 3	Antisense	CAGCAATGTCCTGCATTAACTCAA

[a] Noncoding sequence is shown in lowercase, coding sequence in uppercase.

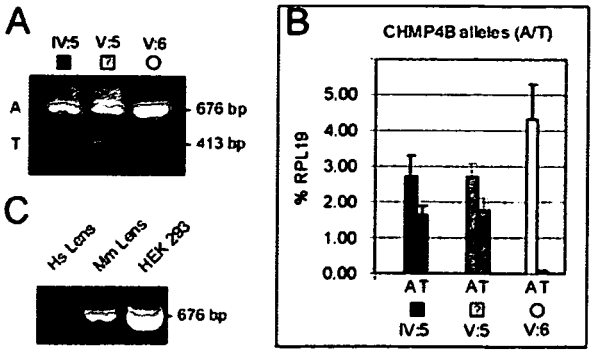

Figure 3. RT-PCR analysis of *CHMP4B* transcripts in peripheral blood leukocytes (PBLs) and eye lens. *A*, Agarose-gel electrophoresis showing nested amplification products of *CHMP4B* transcripts in PBL RNA from family Sk, confirming that individuals IV:5 and V:5 are heterozygous for the mutant T allele (413 bp), whereas individual V:6 is homozygous for the wild-type A allele (676 bp). PBL RNA was purified using the Versagene kit (Gentra), reverse transcribed with the iScript cDNA synthesis kit (Bio-Rad), and PCR amplified as above with three primers (StartF, nested T-alleleR, and EndR) (table 3). *B*, Quantitative amplification of *CHMP4B* transcripts from PBL RNA with allele-specific primers (StartF + A-alleleR, or StartF + T-alleleR) (table 3) showing the relative levels of wild-type (A allele) and mutant (T allele) transcripts in individuals IV:5, V:5, and V:6 from family Sk. RT-PCR products were amplified in a 10-fold dilution series (in triplicate) by use of the iQ SYBR Green Supermix in an iCycler fitted with a MyiQ single-color real-time PCR detection system (Bio-Rad). Allele-specific *CHMP4B* transcripts were detected by melt-curve analysis and standardization against control RPL19 transcript, which was amplified separately in a similar 10-fold dilution series of the same PBL RT-PCR products by use of RPL19 forward (5′-catccgcaagcctgtgac-3′) and reverse (5′-gtgaccttctctggcattcg-3′) primers. *C*, Agarose-gel electrophoresis showing amplicons containing the entire coding region (codons 1–224) of *CHMP4B* transcripts (676 bp) from human (Hs) lens (~30 years old), mouse (Mm) lens (postnatal day 6), and HEK 293 cells. Post mortem human lenses were obtained from the Lions Eye Bank of Oregon, and RNA was extracted using TRIzol reagent (Invitrogen). Following euthanasia (CO_2 gas), mouse lenses were dissected into RNA*later* tissue preservative, and RNA was extracted using the RNAqueous kit (Ambion). RNA was extracted from cultured HEK 293 cells as for mouse lenses. RT-PCR of lens and HEK 293 RNA was performed as for PBL RNA above, with use of StartF and EndR primers (table 3), and the resulting amplicons were verified by sequencing.

within cells and release of Gag into the media as VLPs was detected by immunoblotting (fig. 6*E*). As expected on the basis of previous results,[49] expression of the truncated wild-type fragment (FLAG-CHMP4B$_{1-150}$) inhibited VLP release. Interestingly, the truncated mutant fragment (FLAG-D129V-CHMP4B$_{1-150}$) was a more potent inhibitor than truncated wild type allowing release of only 53% ± 7% (average ± SD) as much Gag in VLPs. Correspondingly, the level of Gag expression in cells expressing the mutant fragment was 1.4 ± 0.3 times that of cells expressing the wild-type fragment. In contrast, neither the wild type nor the mutant forms of full-length CHMP4B significantly inhibited Gag production or VLP release (data not shown).

Precisely how the p.D129V substitution affects the function of CHMP4B is unclear. In this study, we found that the p.D129V substitution changed the subcellular distribution and effects of CHMP4B on VLP release when the protein's acidic C-terminus was removed. Previous studies suggest that the acidic C-termini of CHMPs are regulatory domains that interact specifically with their cognate N-terminal basic domains in an auto-inhibitory manner.[46,49,50] Thus, it is possible that when CHMP4B is relieved from auto-inhibition (mimicked here by truncation), the p.D129V substitution is exposed resulting in deleterious gain-of-function effects. On the basis of expression anal-

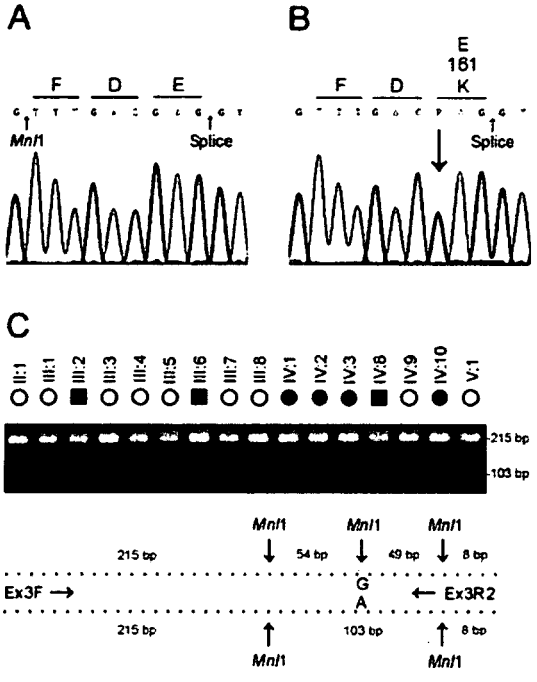

Figure 4. Mutation analysis of *CHMP4B* in the CPP3 family. *A*, Sequence trace of the wild-type allele showing translation of glutamic-acid (E) at codon 161 (GAG). *B*, Sequence trace of the mutant allele showing the heterozygous c.481G→A transition (denoted R by the IUPAC code) that is predicted to result in the missense substitution of lysine (AAG) for glutamate at codon 161 (p.E161K). *C*, Restriction-fragment-length analysis showing loss of an *MnlI* site (3′-GGAGN$_6$) that cosegregates only with affected individuals from the Japanese family[31] heterozygous for the c.481G→A transversion (103 bp). Exon 3 was amplified with PCR primers (table 3) shown in the schematic diagram and resulting amplicons (326 bp) digested (at 37°C for 1 h) with *MnlI* (5 U; New England BioLabs). Restriction fragments (>75 bp) were visualized on 2% agarose-EtBr gels.

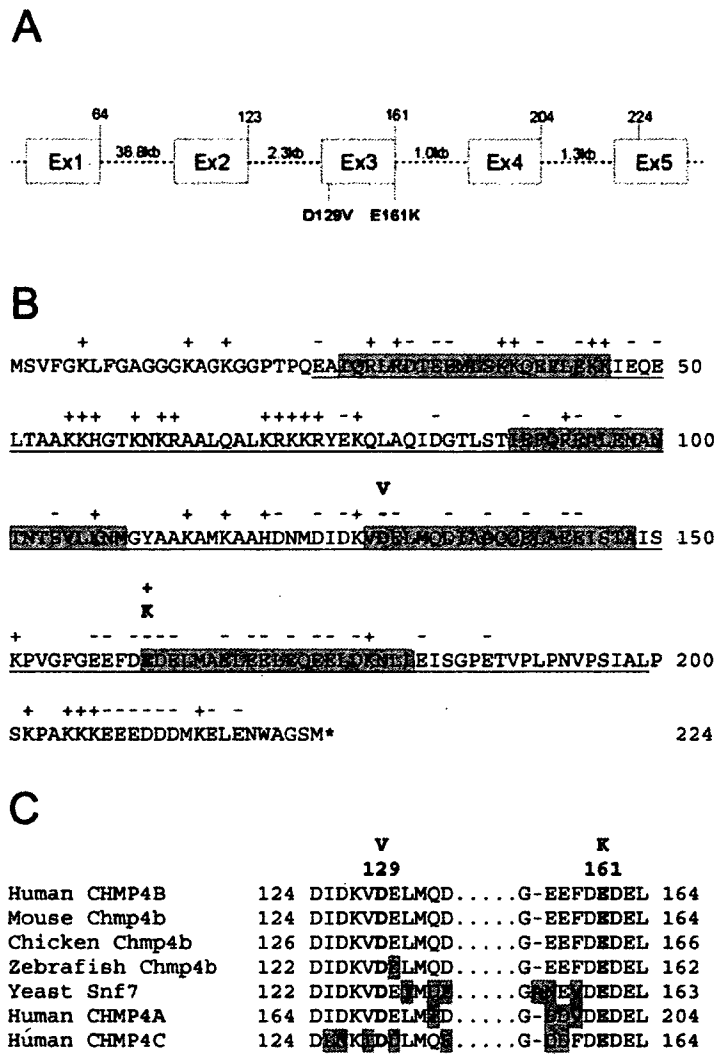

Figure 5. Gene structure and protein domains of CHMP4B. *A*, Exon organization and mutation profile of *CHMP4B*. Intron sizes are indicated (kb), and codons are numbered above each exon. *B*, Amino acid sequence of CHMP4B, showing the conserved SNF7 domain (*underlined*) of this protein family (Conserved Domain Databse, pfam03357) containing at least four predicted helical domains (*grey*). The proposed p.D129V and p.E161K substitutions are predicted to be located in the C-terminal acidic half of the protein, near the start of adjacent helices within the SNF7 domain. Charged amino acids (+, −) and the translation stop codon (*) are also indicated. *C*, Amino acid sequence alignment of human CHMP4B and orthologs from other species, showing phylogenetic conservation of D129 and E161.

ysis of the N-terminal region of CHMP4A,[46] we speculate that, once unmasked, the p.D129V substitution alters the polymerization and/or membrane-binding properties of CHMP4B; however, other mechanisms cannot be excluded. Further work will be required to understand how the p.D129V change affects the behavior of intact CHMP4B. Functional expression studies are also underway to determine how the p.E161K substitution affects CHMP4B. Although little is known about the role of CHMP proteins in lens development, endosome-like compartments have been observed in the newborn mouse lens.[51] Further characterization of endosomal pathways in the lens should provide insight into the pathogenetic mechanisms linking CHMP4B dysfunction with cataractogenesis.

In conclusion, our data identify the first mutations (p.D129V, p.E161K) in a novel gene (*CHMP4B*) for inherited cataracts linked to 20q, and they suggest that gain-of-function defects in an endosome-sorting complex (ESCRT-III) subunit triggers loss of lens transparency.

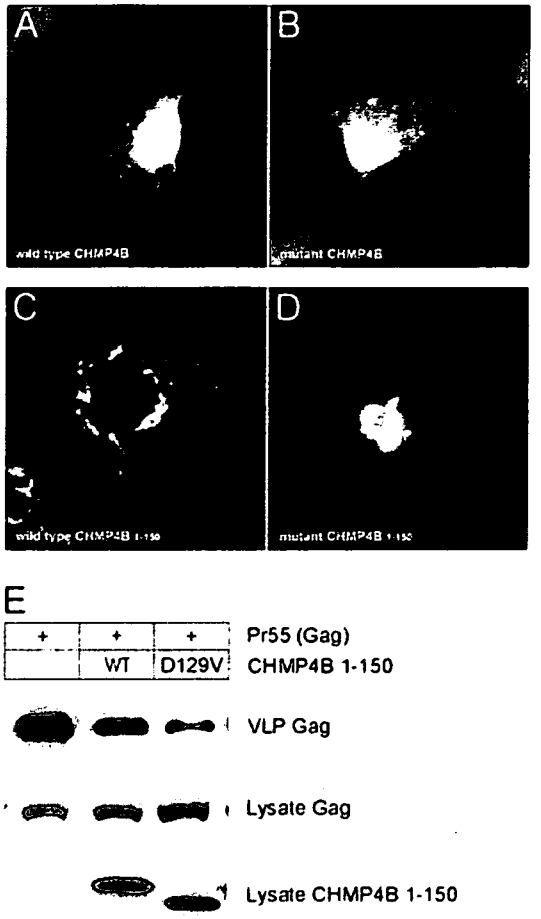

Figure 6. Transient expression of CHMP4B in cultured cells. *A–D*, Subcellular localization of CHMP4B proteins in COS-7 cells, visualized by immunostaining with FLAG antibody and epifluorescence microscopy. *A*, Full-length wild-type FLAG-CHMP4B. *B*, Full-length mutant FLAG-D129V-CHMP4B. *C*, Truncated wild-type FLAG-CHMP4B$_{1-150}$. *D*, Truncated mutant FLAG-D129V-CHMP4B$_{1-150}$. For full-length constructs, the coding sequence (codons 1–224) of human CHMP4B was PCR amplified from HeLa cDNA (Clontech) with forward (5′-gtagatctatgtcggtgt-tcgggaagctgttcgg-3′) and reverse (5′-cactcgagttacatggatccagcccagttctcc-3′) primers and then subcloned into the *Bam*HI and *Xho*I restriction sites in the poly-linker of pcDNA3.1-FLAG.[46] The D129V substitution was generated using the QuickChange mutagenesis kit (Stratagene). For truncated CHMP4B constructs, amplicons corresponding to codons 1–150 were amplified using the full-length constructs as templates and were subcloned into pcDNA3.1-FLAG as above. Plasmid DNA was prepared using the QIAprep spin kit (Qiagen), and inserts were verified by sequencing using the T7 primer. For transient expression, cells were cultured in Dulbecco's modified Eagle's medium (Gibco-BRL) containing 5% fetal bovine serum (Gibco-BRL), 5% supplemented calf serum (Hyclone Laboratories), and 2 mM glutamine. Cells were transfected with expression plasmids by use of Lipofectamine 2000 reagent (Invitrogen). At 18–24 h after transfection, COS-7 cells grown on glass cover slips were fixed in 3.5% paraformaldehyde, permeabilized in 0.2% Triton X-100, and immunostained with rabbit FLAG antibody (Sigma) followed by Alexa Fluor 488 goat anti-rabbit IgG (Molecular Probes). Cell nuclei were counterstained (*blue*) with DAPI (4′,6-Diamidino-2-phenylindole [Molecular Probes]). *E*, Immunoblot analysis of VLPs produced by HEK 293T cells cotransfected with plasmids encoding Gag (p24 antibody) and CHMP4B$_{1-150}$ (FLAG antibody). Top blot shows Gag recovered in VLPs, and middle blot shows Gag in cell lysates. Bottom blot shows that the levels of CHMP4B$_{1-150}$ were similar in cell lysates; however, the D129V substitution increased the electrophoretic mobility of the mutant fragment on SDS (sodium dodecyl sulfate) polyacrylamide gels compared with its wild-type counterpart. For VLPs, HEK 293T cells were transfected with 4 μg pCMV55 encoding HIV Gag, alone or together with 1μg of the indicated CHMP4B construct. At 18–24 h after transfection, media containing VLPs was harvested and clarified by passing through a 0.45 μm filter. VLPs were pelleted by centrifugation (3 h) through a 20% sucrose cushion at 26,000 rpm in SW41 Ti rotor (Beckman Coulter). VLPs and cell lysates were resuspended in sodium dodecyl sulfate (SDS) sample buffer, were separated by SDS-polyacrylamide gel electrophoresis, and then were analyzed by immunoblotting using rabbit antibody against p24, the capsid domain of HIV Gag, horseradish peroxidase (HRP)-conjugated goat anti-rabbit IgG, and the SuperSignal West Pico chemiluminescence detection kit (Pierce). Immunoblot signals were quantified using the Odyssey Infrared Imaging System (Li-Cor Bioscience).

Acknowledgments

We thank family members for participating in this study, Dr. Olivera Boskovska for help with ascertaining family Sk, and Dr. Donna Mackay for preliminary linkage analysis. Dr. Kenneth Johnson kindly provided the pcDNA3.1-FLAG plasmid, and Dr. Lee Ratner kindly provided the HIV GAG expression plasmid (pCMV55) and p24 antibody. This work was supported by National Institutes of Health/National Eye Institute grants EY012284 (to A.S.) and EY02687, and American Heart Association grants 0550148Z and 0750178Z (to P.I.H.).

Web Resources

Accession numbers and URLs for data presented herein are as follows:

ClustalW multiple sequence alignment, http://www.ebi.ac.uk/clustalw/http

Conserved Domain Database (CDD), http://www.ncbi.nlm.nih.gov/Structure/cdd/cdd.shtml

Entrez Protein database, http://www.ncbi.nlm.nih.gov/entrez/query.fcgi?db=Protein

Généthon, Marshfield, and deCODE genetic linkage maps, http://www.ncbi.nlm.nih.gov/genome/guide/human/

LINKAGE/MLINK, http://linkage.rockefeller.edu/soft/

NCBI, http://www.ncbi.nlm.nih.gov/index.html

NCBI Map Viewer, http://www.ncbi.nlm.nih.gov/mapview/

Online Mendelian Inheritance in Man (OMIM), http://www.ncbi.nlm.nih.govOMIM

SNP database (dbSNP), http://www.ncbi.nlm.nih.gov/projects/SNP/

UniGene, http://www.ncbi.nlm.nih.gov/entrez/query.fcgi?db=unigene

References

1. Zetterstrom C, Lundvall A, Kugelberg M (2005) Cataracts in children. J Cataract Refract Surg 31:824–840
2. Shiels A, Hejtmancik JF (2007) Genetic origins of cataract. Arch Ophthalmol 125:165–173
3. Litt M, Kramer P, LaMorticella DM, Murphey W, Lovrien EW, Weleber RG (1998) Autosomal dominant congenital cataract associated with a missense mutation in the human alpha crystallin gene CRYAA. Hum Mol Genet 7:471–474
4. Berry V, Francis P, Reddy MA, Collyer D, Vithana E, MacKay I, Dawson G, Carey AH, Moore A, Bhattacharya SS, et al (2001) Alpha-B crystallin gene (CRYAB) mutation causes dominant congenital posterior polar cataract in humans. Am J Hum Genet 69:1141–1145
5. Mackay DS, Boskovska OB, Knopf HL, Lampi KJ, Shiels A (2002) A nonsense mutation in CRYBB1 associated with autosomal dominant cataract linked to human chromosome 22q. Am J Hum Genet 71:1216–1221
6. Litt M, Carrero-Valenzuela R, LaMorticella DM, Schiltz DW, Mitchell TN, Kramer P, Maumenee IH (1997) Autosomal dominant cerulean cataract is associated with a chain termination mutation in the human β-crystallin gene CRYBB2. Hum Mol Genet 6:665–668
7. Riazuddin SA, Yasmeen A, Yao W, Sergeev YV, Zhang Q, Zulfigar F, Riaz A, Riazuddin S, Hejtmancik JF (2005) Mutations in βB3-crystallin associated with autosomal recessive cataract in two Pakistani families. Invest Ophthalmol Vis Sci 46:2100–2106
8. Kannabiran C, Rogan PK, Olmos L, Basti S, Rao GN, Kaiser-Kupfer M, Hejtmancik JF (1998) Autosomal dominant zonular cataract with sutural opacities is associated with a splice mutation in the βA3/A1-crystallin gene. Mol Vis 4:21
9. Billingsley G, Santhiya ST, Paterson AD, Ogata K, Wodak S, Hosseni SM, Manisastry SM, Vijayalakshmi P, Gopinath PM, Graw J, et al (2006) *CRYBA4* a novel human cataract gene is also involved in microphthalmia. Am J Hum Genet 79:702–709
10. Santhiya ST, Shyam Manohar M, Rawlley D, Vijayalakshmi P, Namperumalsamy P, Gopinath PM, Loster J, Graw J (2002) Novel mutations in the γ-crystallin genes cause autosomal dominant congenital cataracts. J Med Genet 39:352–358
11. Sun H, Ma Z, Li Y, Liu B, Li Z, Ding X, GaoY, Ma W, Tang X, Li X, et al (2005) Gamma-S crystallin gene (CRYGS) mutation causes dominant progressive cortical cataract in humans. J Med Genet 42:706–710
12. Mackay D, Ionides A, Kibar Z, Rouleau G, Berry V, Moore A, Shiels A, Bhattacharya S (1999) Connexin46 mutations in autosomal dominant congenital cataract. Am J Hum Genet 64:1357–1364
13. Shiels A, Mackay D, Ionides A, Berry V, Moore A, Bhattacharya S (1998) A missense mutation in the human connexin50 gene (*GJA8*) underlies autosomal dominant zonular pulverulent cataract on chromosome 1q. Am J Hum Genet 62:526–532
14. Bu L, Jin Y, Shi Y, Chu R, Ban A, Eiberg H, Andres L, Jiang H, Zheng G, Qian M, et al (2002) Mutant DNA binding domain of HSF4 is associated with autosomal dominant lamellar and Marner cataract. Nat Genet 31:276–278
15. Berry V, Francis P, Kaushal S, Moore A, Bhattacharya S (2000) Missense mutations in *MIP* underlie autosomal dominant polymorphic and lamellar cataracts linked to 12q. Nat Genet 25:15–17
16. Pras E, Levy-Nissenbaum E, Bakhan T, Lahat H, Assia E, Geffin-Carmi N, Frydman M, Goldman B, Pras E (2002) A missense mutation in the *LIM2* gene is associated with autosomal recessive presenile cataract in an inbred Iraqi Jewish family. Am J Hum Genet 70:1363–1367
17. Ramachandran RD, Perumalsamy V, Hejtmancik JF (2007) Autosomal recessive juvenile onset cataract associated with mutation in *BFSP1*. Hum Genet 121:475–482
18. Conley YP, Erturk D, Keverline A, Mah TS, Keravala A, Barnes LR, Bruchis A, Hess JF, FitzGerald PG, Weeks DE, et al (2000) A juvenile-onset progressive cataract locus on chromosome 3q21-q22 is associated with a missense mutation in the beaded filament structural protein-2. Am J Hum Genet 66:1426–1431
19. Eiberg H, Lund AM, Warburg M, Rosenberg T (1995) Assignment of congenital cataract Volkmann type (CCV) to chromosome 1p36. Hum Genet 96:33–38
20. Ionides ACW, Berry V, Mackay DS, Moore AT, Bhattacharya SS, Shiels A (1997) A locus for autosomal dominant posterior polar cataract on chromosome 1p. Hum Mol Genet 6:47–51
21. McKay JD, Patterson B, Craig JE, Russell-Eggitt IM, Wirth MG, Burdon KP, Hewitt AW, Cohn AC, Kerdraon Y, Mackey DA (2005) The telomere of human chromosome 1p contains at least two independent autosomal dominant congenital cataract genes. Br J Ophthalmol 89:831–834
22. Rogaev EI, Rogaeva EA, Korovaitseva GI, Farrer LA, Petrin AN, Keryanov SA, Turaeva S, Chumakov I, St George-Hyslop P, Ginter EK (1996) Linkage of polymorphic congenital cataract

to the gamma-crystallin gene locus on human chromosome 2q33–35. Hum Mol Genet 5:699–703
23. Khaliq S, Hameed A, Ismail M, Anwar K, Mehdi SQ (2002) A novel locus for autosomal dominant nuclear cataract mapped to chromosome 2p12 in a Pakistani family. Invest Ophthalmol Vis Sci 43:2083–2087
24. Gao L, Qin W, Cui H, Feng G, Liu P, Gao W, Ma L, Li P, He L, Fu S (2005) A novel locus of coralliform cataract mapped to chromosome 2p24-pter. J Hum Genet 50:305–310
25. Pras E, Pras E, Bakhan T, Levy-Nissenbaum E, Lahat H, Assia EI, Garzozi HJ, Kastner DL, Goldman B, Frydman M (2001) A gene causing autosomal recessive cataract maps to the short arm of chromosome 3. Isr Med Assoc J 3:559–562
26. Heon E, Paterson AD, Fraser M, Billingsley G, Priston M, Balmer A, Schorderet DF, Verner A, Hudson TJ, Munier FL (2001) A progressive autosomal recessive cataract locus maps to chromosome 9q13-q22. Am J Hum Genet 68:772–777
27. Vanita, Singh JR, Sarhadi VK, Singh D, Reis A, Rueschendorf F, Becker-Follmann J, Jung M, Sperling K (2001) A novel form of central pouchlike cataract with sutural opacities maps to chromosome 15q21-22. Am J Hum Genet 68:509–514
28. Armitage MM, Kivlin JD, Ferrell RE (1995) A progressive early onset cataract gene maps to human chromosome 17q24. Nat Genet 9:37–40
29. Berry V, Ionides AC, Moore AT, Plant C, Bhattacharya SS, Shiels A (1996) A locus for autosomal dominant anterior polar cataract on chromosome 17p. Hum Mol Genet 5:415–419
30. Riazuddin SA, Yasmeen A, Zhang Q, Yao W, Sabar MF, Ahmed Z, Riazuddin S, Hejtmancik JF (2005) A new locus for autosomal recessive nuclear cataract mapped to chromosome 19q13 in a Pakistani family. Invest Ophthalmol Vis Sci 46: 623–626
31. Yamada K, Tomita H, Yoshiura K, Kondo S, Wakui K, Fukushima Y, Ikegawa S, Nakamura Y, Amemiya T, Niikawa N (2000) An autosomal dominant posterior polar cataract locus maps to human chromosome 20p12-q12. Eur J Hum Genet 8:535–539
32. Li N, Yang Y, Bu J, Zhao C, Lu S, Zhao J, Yan L, Cui L, Zheng R, Li J, et al (2006) An autosomal dominant progressive congenital zonular nuclear cataract linked to chromosome 20p12.2-p11.23. Mol Vis 12:1506–1510
33. Mackay DS, Andley UP, Shiels A (2003) Cell death triggered by a novel mutation in the alphaA-crystallin gene underlies autosomal dominant cataract linked to chromosome 21q. Eur J Hum Genet 11:784–793
34. Lathrop GM, Lalouel JM, Julier C, Ott J (1984) Strategies for multilocus linkage analysis in humans. Proc Natl Acad Sci USA 81:3443–3446
35. Katoh K, Shibata H, Hatta K, Maki M (2004) CHMP4b is a major binding partner of the ALG-2-interacting protein Alix among the three CHMP4 isoforms. Arch Biochem Biophys 421:159–165
36. Cartegni L, Chew SL, Krainer AR (2002) Listening to silence and understanding nonsense: exonic mutations that affect splicing. Nat Rev Genet 3:285–298
37. Yamada K, Tomita HA, Kanazawa S, Mera A, Amemiya T, Niikawa N (2000) Genetically distinct autosomal dominant posterior polar cataract in a four-generation Japanese family. Am J Ophthalmol 129:159–165
38. West JD, Fisher G (1986) Further experience of the mouse dominant cataract mutation test from an experiment with ethylnitrosourea. Mutat Res 164:127–136
39. Hurley JH, Emr SD (2006) The ESCRT complexes: structure and mechanism of a membrane-trafficking network. Annu Rev Biophys Biomol Struct 35:277–298
40. Horii M, Shibata H, Kobayashi R, Katoh K, Yorikawa C, Yasuda J, Maki M (2006) CHMP7 a novel ESCRT-III related protein associates with CHMP4b and functions in the endosomal sorting pathway. Biochem J 400:23–32
41. Skibinski G, Parkinson NJ, Brown JM, Chakrabarti L, Lloyd SL, Hummerich H, Nielsen JE, Hodges JR, Spillantini MG, Thursgaard T, et al (2005) Mutations in the endosomal ESCRT-III complex subunit CHMP2B in frontotemporal dementia. Nat Genet 37:806–808
42. Parkinson N, Ince PG, Smith MO, Highley R, Skibinski G, Andersen PM, Morrison KE, Pall HS, Hardiman O, Collinge J, et al (2006) ALS phenotypes with mutations in CHMP2B (charged multivesicular body protein 2B). Neurology 67: 1074–1077
43. Talbot K, Ansorge O (2006) Recent advances in the genetics of amyotrophic lateral sclerosis and frontotemporal dementia: common pathways in neurodegenerative disease. Hum Mol Genet 15:R182–R187
44. Katoh K, Shibata H, Suzuki H, Nara A, Ishidoh K, Kominami E, Yoshimori T, Maki M (2003) The ALG-2-interacting protein Alix associates with CHMP4b a human homologue of yeast Snf7 that is involved in multivesicular body sorting. J Biol Chem 278:39104–39113
45. von Schwedler UK, Stuchell M, Muller B, Ward DM, Chung HY, Morita E, Wang HE, Davis T, He GP, Cimbora DM, et al (2003) The protein network of HIV budding. Cell 114:701–713
46. Lin Y, Kimpler LA, Naismith TV, Lauer JM, Hanson PI (2005) Interaction of the mammalian endosomal sorting complex required for transport (ESCRT) III protein hSnf7-1 with itself membranes and the AAA+ ATPase SKD1. J Biol Chem 280: 12799–12809
47. Muziol T, Pineda-Molina E, Ravelli RB, Zamborlini A, Usami Y, Gottlinger H, Weissenhorn W (2006) Structural basis for budding by the ESCRT-III factor CHMP3. Dev Cell 10:821–830
48. Accola MA, Strack B, Gottlinger HG (2000) Efficient particle production by minimal Gag constructs which retain the carboxy-terminal domain of human immunodeficiency virus type 1 capsid-p2 and a late assembly domain. J Virol 74:5395–5402
49. Zamborlini A, Usami Y, Radoshitzky SR, Popova E, Palu G, Gottlinger H (2006) Release of autoinhibition converts ESCRT-III components into potent inhibitors of HIV-1 budding. Proc Natl Acad Sci USA 103:19140–19145
50. Whitley P, Reaves BJ, Hashimoto M, Riley AM, Potter BVL, Holman GD (2003) Identification of mammalian Vps24p as an effector of phosphatidylinositol 3,5-bisphosphate-dependent endosome compartmentalization. J Biol Chem 278: 38786–38795
51. Beebe D, Garcia C, Wang X, Rajagopal R, Feldmeier M, Kim J-Y, Chytil A, Moses H, Ashery-Padan R, Rauchman M (2004) Contributions by members of the TGFbeta superfamily to lens development. Int J Dev Biol 48:845–856

Mutations in CD96, a Member of the Immunoglobulin Superfamily, Cause a Form of the C (Opitz Trigonocephaly) Syndrome

Tadashi Kaname, Kumiko Yanagi, Yasutsugu Chinen, Yoshio Makita, Nobuhiko Okamoto, Hiroki Maehara, Ichiro Owan, Fuminori Kanaya, Yoshiaki Kubota, Yuichi Oike, Toshiyuki Yamamoto, Kenji Kurosawa, Yoshimitsu Fukushima, Axel Bohring, John M. Opitz, Ko-ichiro Yoshiura, Norio Niikawa, and Kenji Naritomi

The C syndrome is characterized by trigonocephaly and associated anomalies, such as unusual facies, psychomotor retardation, redundant skin, joint and limb abnormalities, and visceral anomalies. In an individual with the C syndrome who harbors a balanced chromosomal translocation, t(3;18)(q13.13;q12.1), we discovered that the *TACTILE* gene for CD96, a member of the immunoglobulin superfamily, was disrupted at the 3q13.3 breakpoint. In mutation analysis of nine karyotypically normal patients given diagnoses of the C or C-like syndrome, we identified a missense mutation (839C→T, T280M) in exon 6 of the *CD96* gene in one patient with the C-like syndrome. The missense mutation was not found among 420 unaffected Japanese individuals. Cells with mutated CD96 protein (T280M) lost adhesion and growth activities in vitro. These findings indicate that CD96 mutations may cause a form of the C syndrome by interfering with cell adhesion and growth.

The C (Opitz trigonocephaly) syndrome (MIM %211750) is a malformation syndrome of unknown cause, and its mode of inheritance has been suggested to be autosomal recessive. The syndrome comprises trigonocephaly and associated anomalies, such as unusual facies, wide alveolar ridges, multiple buccal frenula, limb defects, visceral anomalies, redundant skin, psychomotor retardation, and hypotonia.[1,2]

Recently, Bohring et al.[3,4] suggested the delineation or existence of a severe form of the C syndrome (the C-like syndrome, or Bohring-Opitz syndrome [MIM 605039]). More recently, Osaki et al.[5] reported on a newborn infant who had many clinical features similar to those of the C-like syndrome but did not have exophthalmoses, which has been regarded as a hallmark of the C-like syndrome. They suggested that the manifestations in this patient are a further indication of overlap between the C-like syndrome and the C syndrome. Thus, it is controversial whether there is (1) a gradient of spectrum in the C syndrome, from the mild form (C syndrome) to the severe form (C-like syndrome), or (2) genetic heterogeneity among the patients with the C syndrome.

In addition, various chromosomal abnormalities, especially those that include chromosome 3, have been reported in patients originally described as having the C syndrome.[2] These include 3p monosomy,[6] distal 3p trisomy,[7] 3q trisomy,[8] distal 3q trisomy with deletion of distal 3p,[9] and inversion in chromosome 3.[10] Although these cases might be removed from the C syndrome because they involve chromosome abnormalities, it is possible that there could be putative genes (or multiple loci) related to trigonocephaly and, even further, to pathogenesis of the C syndrome in chromosome 3.[2,10]

We encountered a boy with the C syndrome and a de novo balanced translocation, 46,XY,t(3;18)(q13.13;q12.1).[11] By construction of a BAC/cosmid contig covering the breakpoints, we found the *CD96* (*TACTILE*) gene (GenBank accession number NM_198196) encoding a member of the immunoglobulin superfamily[12] at the 3q13.13 breakpoint (fig. 1*A*). The *CD96* gene consists of 15 exons and spans ~120 kb in the genome. Precise structural analysis around the breakpoint showed that the gene was disrupted by the translocation in exon 5, probably leading to premature termination or loss of expression of CD96 protein. There is no gene or poly-A signal in a 500-kb region telomeric to the breakpoint of chromosome 18, according to the Ensembl Genome Browser Web site. FISH analysis with use of a BAC clone, RP11-158B11, demon-

Departments of Medical Genetics (T.K.; K.Y.; K.N.), Pediatrics (Y.C.), and Orthopedics (H.M.; I.O.; F.K.), University of the Ryukyus Faculty of Medicine, Nishihara, Japan; Department of Pediatrics, Asahikawa Medical College, Asahikawa, Japan (Y.M.); Department of Developmental Medicine, Osaka Medical Center and Research Institute for Maternal and Child Health, Izumi, Japan (N.O.); Department of Cell Differentiation, Keio University School of Medicine, Tokyo (Y.K.; Y.O.); Division of Medical Genetics, Kanagawa Children's Medical Center, Yokohama, Japan (T.Y.; K.K.); Department of Medical Genetics, Shinshu University School of Medicine, Matsumoto, Japan (Y.F.); Institut für Humangenetik, Westfälische Wilhelms-Universität, Münster, Germany (A.B.); Department of Pediatrics, Pathology, Obstetrics and Gynecology, and Human Genetics, University of Utah School of Medicine, Salt Lake City (J.M.O.); Department of Human Genetics, Nagasaki University Graduate School of Biomedical Sciences, Nagasaki, Japan (K-i.Y.; N.N.); and Solution Oriented Research for Science and Technology (SORST), Japan Science and Technology, Kawaguchi, Japan (T.K.; Y.F.; K-i.Y.; N.N.; K.N.)

Received January 24, 2007; accepted for publication June 14, 2007; electronically published August 27, 2007.

Address for correspondence and reprints: Dr. Tadashi Kaname, Department of Medical Genetics, University of the Ryukyus Faculty of Medicine, 207 Uehara, Nishihara, Okinawa 903-0215, Japan. E-mail: tkaname@med.u-ryukyu.ac.jp

Am. J. Hum. Genet. 2007;81:835–841. 0002-9297/2007/8104-0027$15.00
DOI: 10.1086/522014

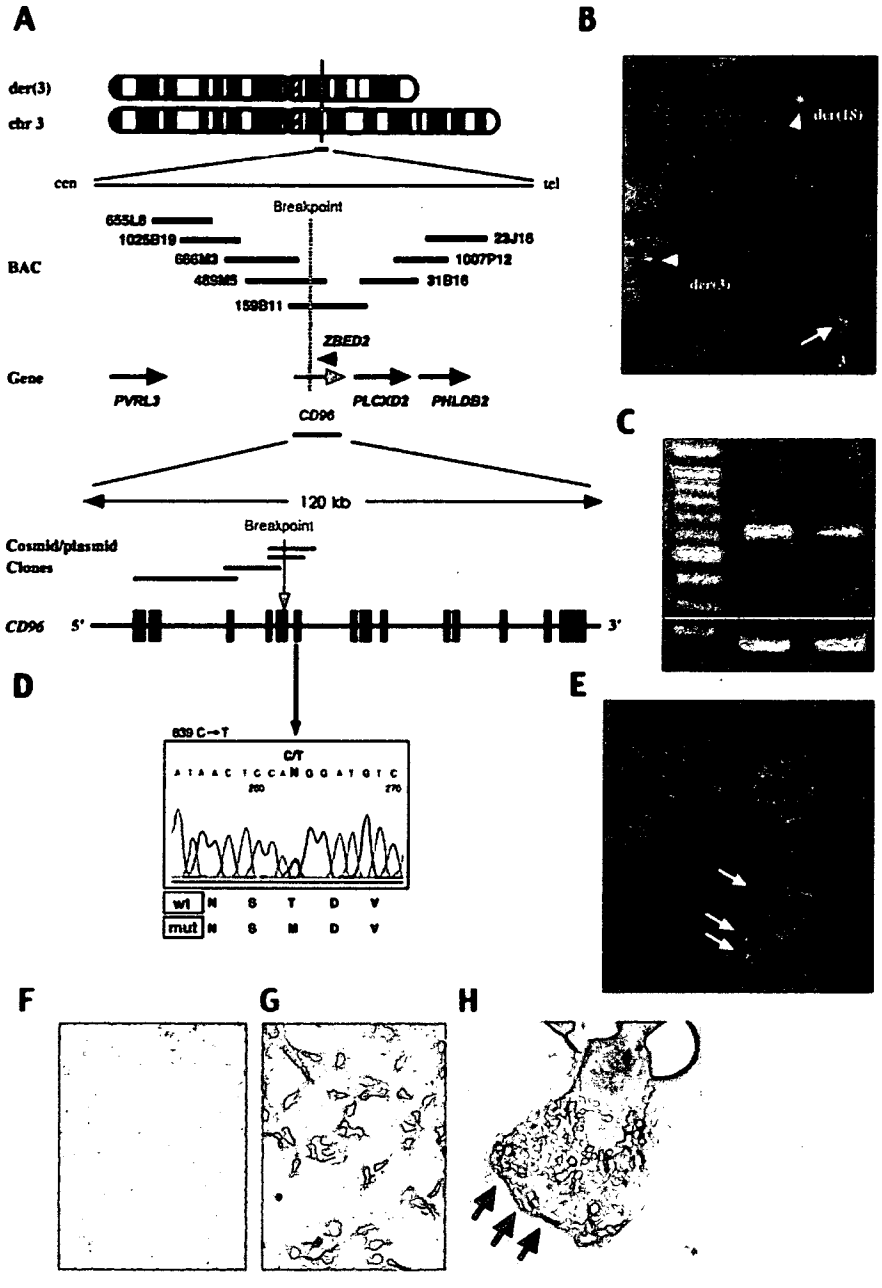

Figure 1. CD96 mutations in the C or C-like syndrome and its expression. *A*, BAC and cosmid/plasmid map spanning the 3q13.3 breakpoint of a patient with a translocation, t(3;18)(q13.13;q12.1). The red vertical line and dashed red line indicate the breakpoint. Blue bars for BACs or plasmids indicate clones covering the breakpoint (detected by FISH analysis). A red horizontal arrow indicates the *CD96* gene. A red vertical arrow indicates the breakpoint in the *CD96* gene. *B*, FISH analysis of the patient harboring the translocation. FISH signals for BAC RP11-159B11 are separated into two chromosomes, der(3) and der(18), whose signals are indicated by arrowheads. An arrow indicates signals on a normal chromosome 3. *C*, RT-PCR for *CD96* expression in the B cells of an unaffected individual and the patient with C syndrome. The left, middle, and right lanes depict a 100-bp ladder, an unaffected control, and the patient with C syndrome with translocation, respectively. The lower panel indicates expression of *GAPDH* as the control. *D*, Direct DNA-sequence analysis of *CD96* demonstrates a point mutation in a patient. *E–H*, Immunocytochemical analysis for CD96 localization in HT1080 cells with use of rabbit anti-CD96 antibody and FITC-conjugated (*E*) or HRP-conjugated (*G–H*) goat anti-rabbit IgG. *E*, Counterstained with 4′,6-diamidino-2-phenylindole (original magnification 400×). *F–H*, Counterstained with methyl green. *F*, Negative control. Original magnification was 100× (*F* and *G*) or 400× (*H*). White arrows (*E*) and black arrows (*H*) indicate regions adherent to the plastic dish.